(12) INTERNATIONAL APPLICATION PUBLISHED UNDER THE PATENT COOPERATION TREATY (PCT)

(19) World Intellectual Property Organization
International Bureau

(43) International Publication Date
6 December 2001 (06.12.2001)

PCT

(10) International Publication Number
WO 01/92381 A1

(51) International Patent Classification[7]: C08J 5/04, 5/06

(21) International Application Number: PCT/US00/33291

(22) International Filing Date: 7 December 2000 (07.12.2000)

(25) Filing Language: English

(26) Publication Language: English

(30) Priority Data:
60/169,273 7 December 1999 (07.12.1999) US

(71) Applicant *(for all designated States except US)*: **WILLIAM MARSH RICE UNIVERSITY** [US/US]; Office of Technology Transfer-MS705, 6100 Main Street, Houston, TX 77005-1892 (US).

(72) Inventors; and

(75) Inventors/Applicants *(for US only)*: **BARRERA, Enrique, V.** [US/US]; 15 Sunset Boulevard, Houston, TX 77005 (US). **RODRIGUEZ, Fernando, J.** [US/US]; Apartment 1044, 4010 Linkwood Drive, Houston, TX 77025 (US). **LOZANO, Karen** [US/US]; 1201 West University Drive, Edinburg, TX 78539-2999 (US). **CHIBANTE, Luis, Paulo, Felipe** [US/US]; 11503 Piping Rock Lane, Houston, TX 77077 (US). **STEWART, David, Harris** [US/US]; 1260 Shotwell Road, Houston, TX 77020 (US).

(74) Agent: **SHADDOX, Robert, C.**; Winstead Sechrest & Minick, 2400 Bank One Center, 910 Travis Street, Houston, TX 77002-5895 (US).

(81) Designated States *(national)*: AE, AG, AL, AM, AT, AU, AZ, BA, BB, BG, BR, BY, BZ, CA, CH, CN, CR, CU, CZ, DE, DK, DM, DZ, EE, ES, FI, GB, GD, GE, GH, GM, HR, HU, ID, IL, IN, IS, JP, KE, KG, KP, KR, KZ, LC, LK, LR, LS, LT, LU, LV, MA, MD, MG, MK, MN, MW, MX, MZ, NO, NZ, PL, PT, RO, RU, SD, SE, SG, SI, SK, SL, TJ, TM, TR, TT, TZ, UA, UG, US, UZ, VN, YU, ZA, ZW.

(84) Designated States *(regional)*: ARIPO patent (GH, GM, KE, LS, MW, MZ, SD, SL, SZ, TZ, UG, ZW), Eurasian patent (AM, AZ, BY, KG, KZ, MD, RU, TJ, TM), European patent (AT, BE, CH, CY, DE, DK, ES, FI, FR, GB, GR, IE, IT, LU, MC, NL, PT, SE, TR), OAPI patent (BF, BJ, CF, CG, CI, CM, GA, GN, GW, ML, MR, NE, SN, TD, TG).

Published:
— *with international search report*

For two-letter codes and other abbreviations, refer to the "Guidance Notes on Codes and Abbreviations" appearing at the beginning of each regular issue of the PCT Gazette.

(54) Title: ORIENTED NANOFIBERS EMBEDDED IN POLYMER MATRIX

(57) Abstract: A method of forming a composite of embedded nanofibers in a polymer matrix is disclosed. The method includes incorporating nanofibers in a plastic matrix forming agglomerates, and uniformly distributing the nanofibers by exposing the agglomerates to hydrodynamic stresses. The hydrodynamic said stresses force the agglomerates to break apart. In combination or additionally elongational flow is used to achieve small diameters and alignment. A nanofiber reinforced polymer composite system is disclosed. The system includes a plurality of nanofibers that are embedded in polymer matrices in micron size fibers. A method for producing nanotube continuous fibers is disclosed. Nanofibers are fibrils with diameters 100 nm, multiwall nanotubes, single wall nanotubes and their various functionalized and derivatized forms. The method includes mixing a nanofiber in a polymer; and inducing an orientation of the nanofibers that enables the nanofibers to be used to enhance mechanical, thermal and electrical properties. Orientation is induced by high shear mixing and elongational flow, singly or in combination. The polymer may be removed from said nanofibers, leaving micron size fibers of aligned nanofibers.

WO 01/92381 A1

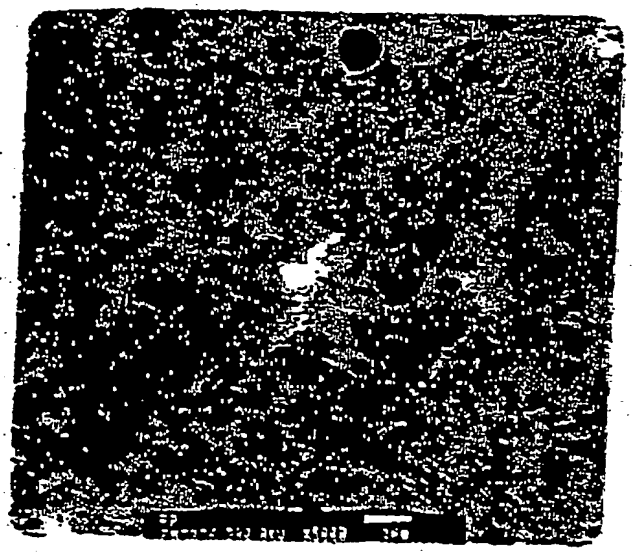

Figure 2 TEM micrograph

FIGURE 3 SEM micrographs

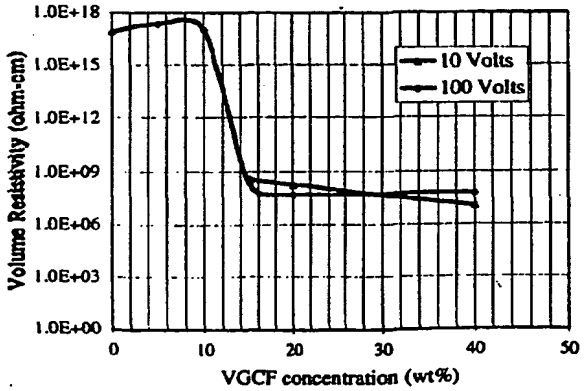

Figure 1a Volume resistivity

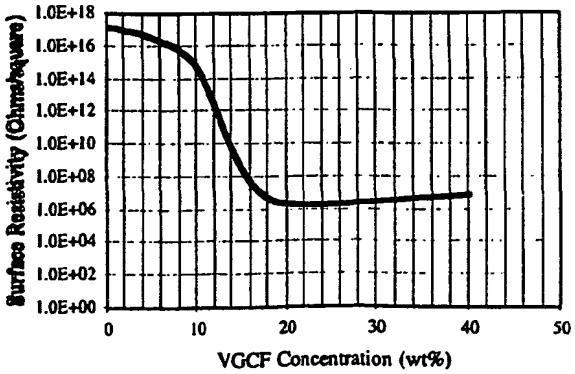

Figure 1b Surface resisitivity

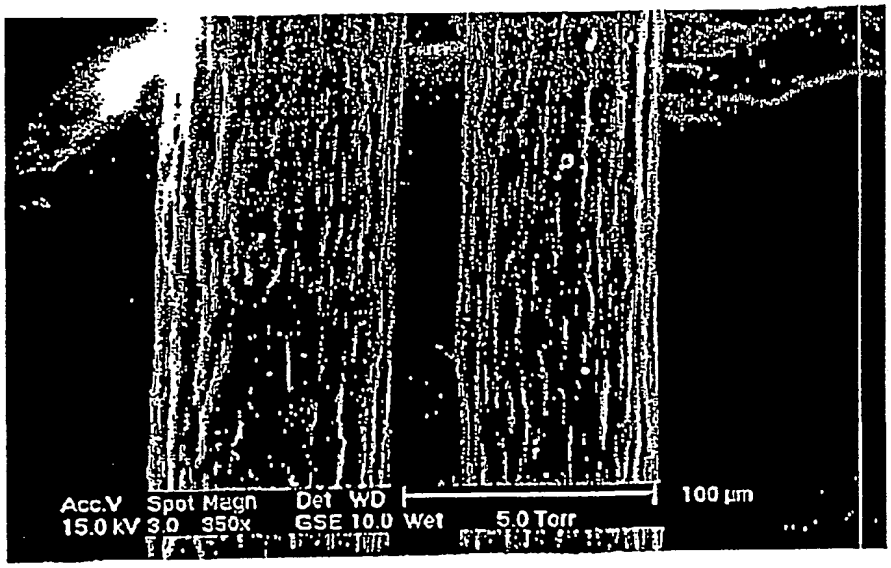

Figure 4. Comparison of two micron size fiber composite diameters.

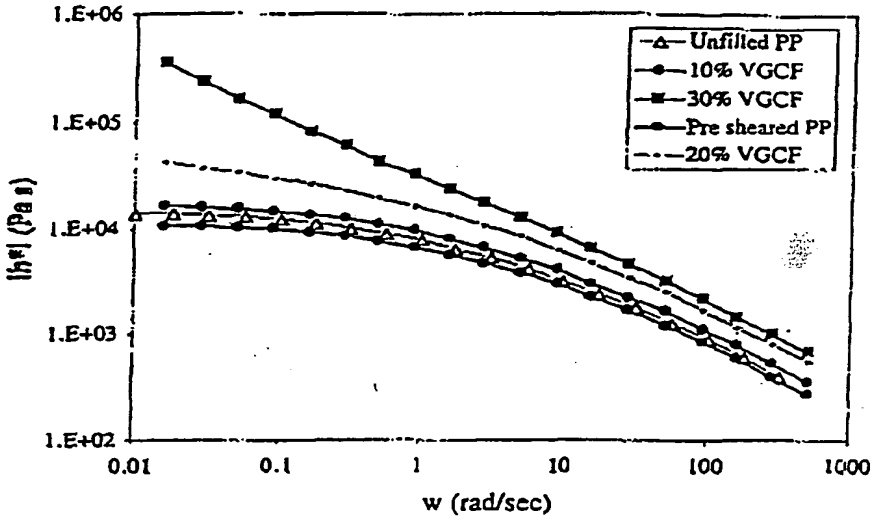

Figure 5. Viscosity vs. shear rate

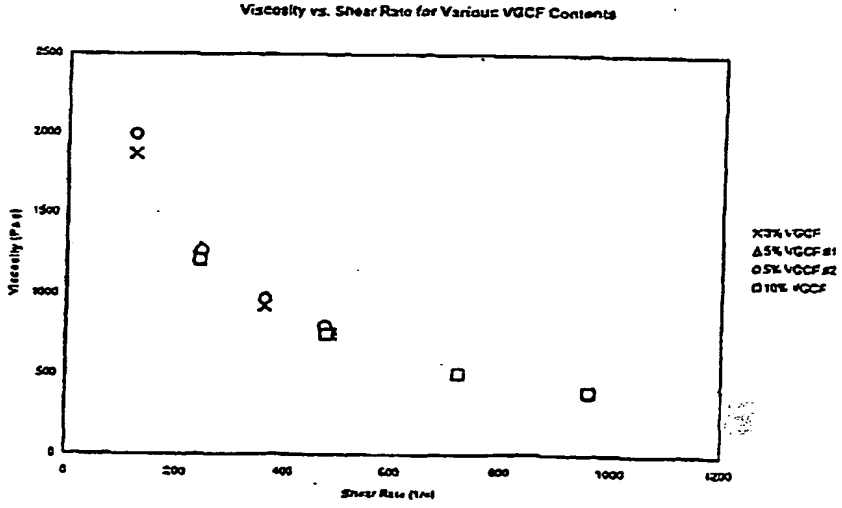

Figure 6. Change in viscosity with increasing shear rate for a 5 wt.% VGCF-PE system.

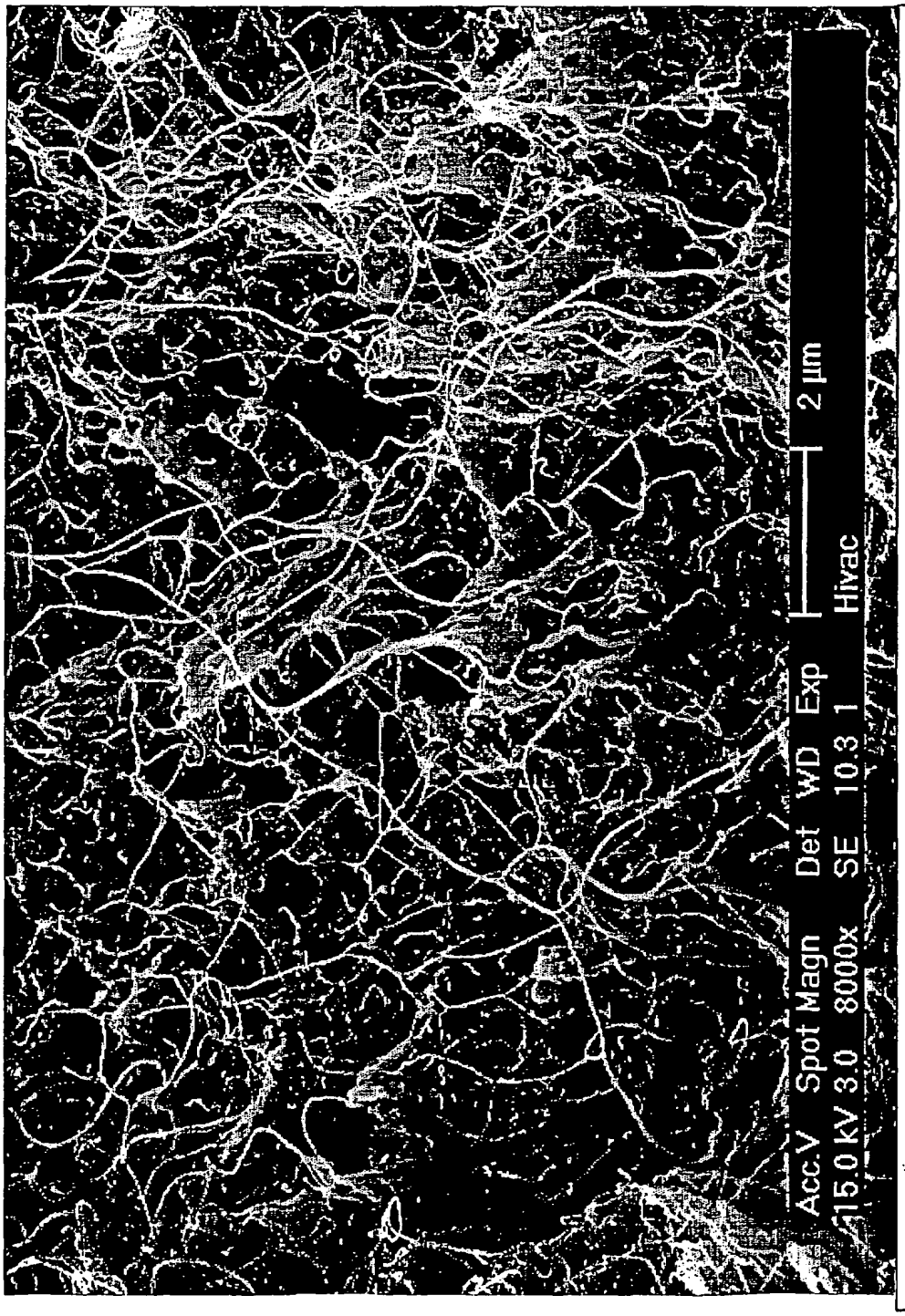

Figure 4 | A micrograph of a 10 wt.% SWNT/ABS polymer which was fractured at room temperature. Note the good dispersion, the absence of porosity, and the reduced entanglement of the nanotubes.

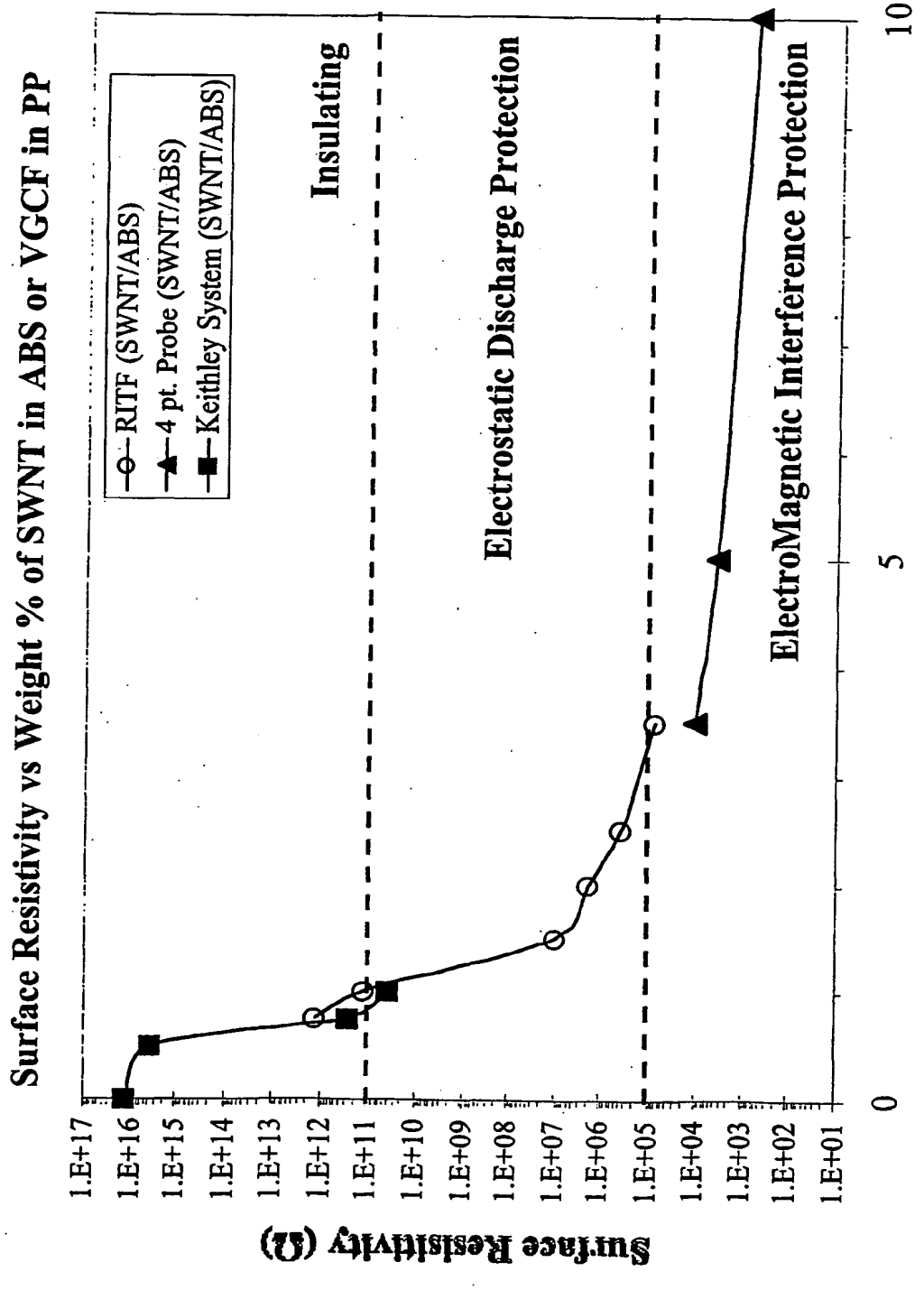

Figure 7 Surface Resistivity for ABS as a function of SWNT composition

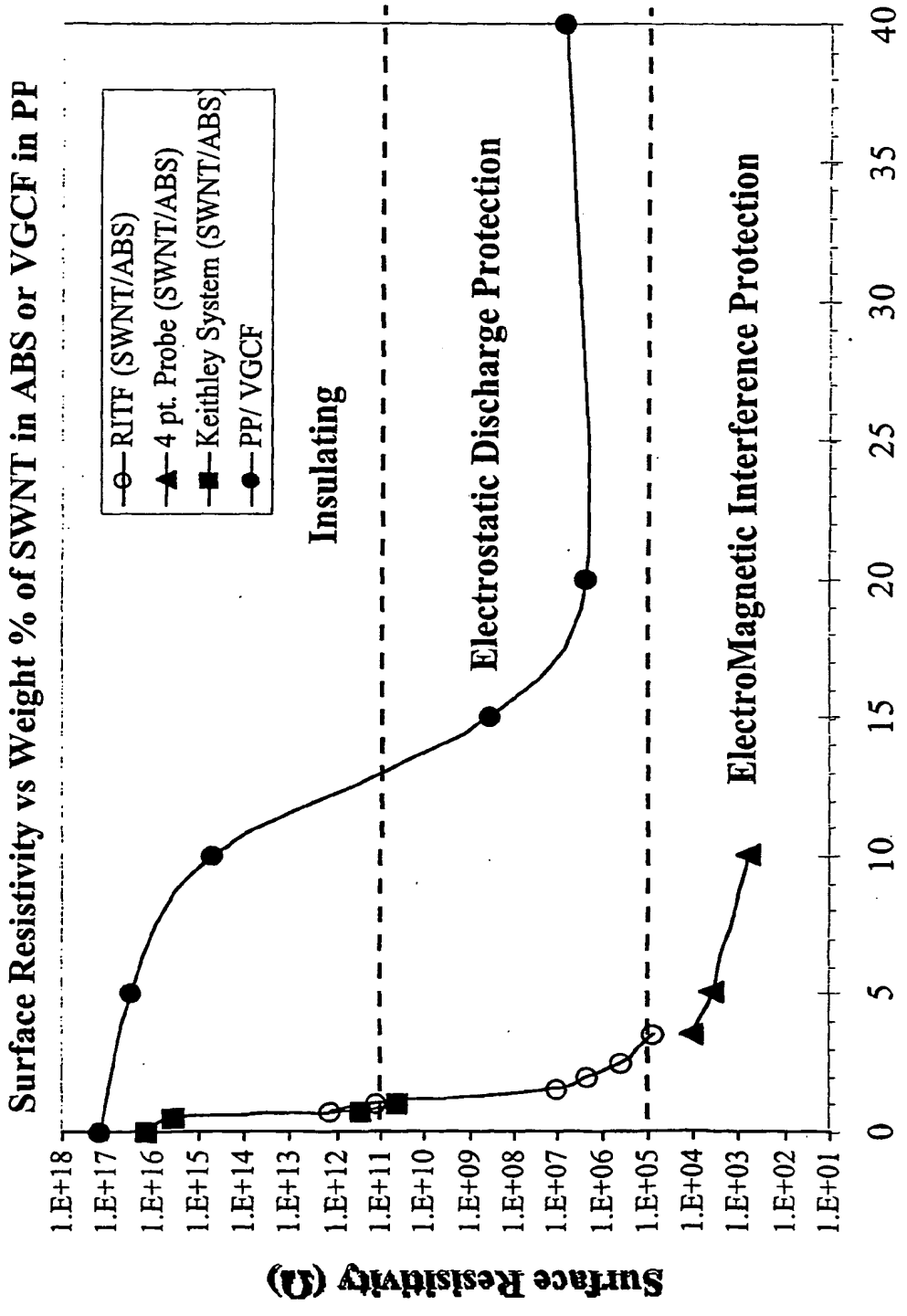
Surface Resistivity vs Weight % of SWNT in ABS or VGCF in PP
RITF (SWNT/ABS)
4 pt. Probe (SWNT/ABS)
Keithley System (SWNT/ABS)
PP/ VGCF
Insulating
Electrostatic Discharge Protection
ElectroMagnetic Interference Protection
Surface Resistivity (Ω)
1.E+18
1.E+17
1.E+16
1.E+15
1.E+14
1.E+13
1.E+12
1.E+11
1.E+10
1.E+09
1.E+08
1.E+07
1.E+06
1.E+05
1.E+04
1.E+03
1.E+02
1.E+01
0
5
10
15
20
25
30
35
40
Weight %

Figure 8.

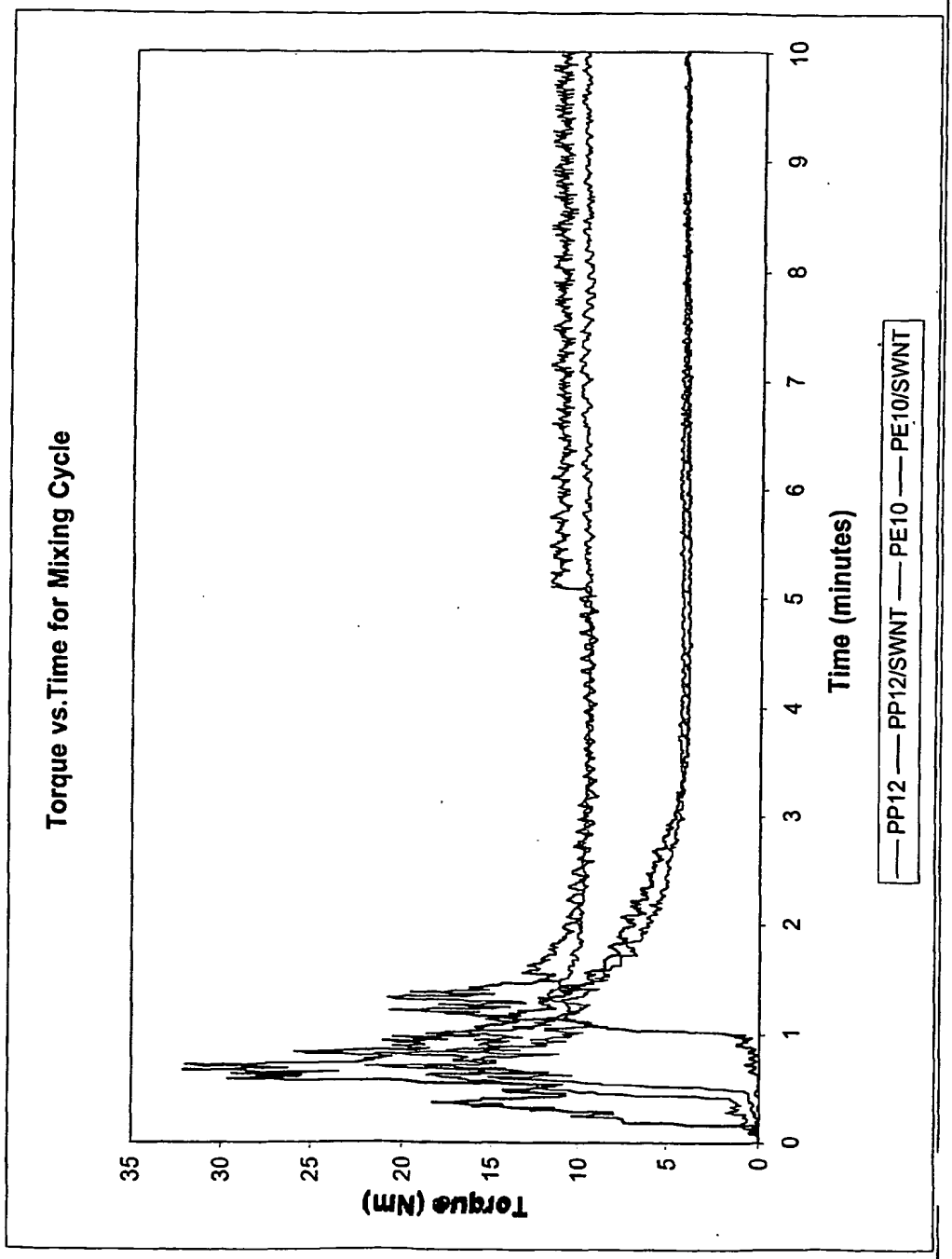

Figure 10 Torque data for the PP12 and PE10 polymer systems which show very low values or torque indicating that mixing has no problems with excessive viscosity as seen by other investigators

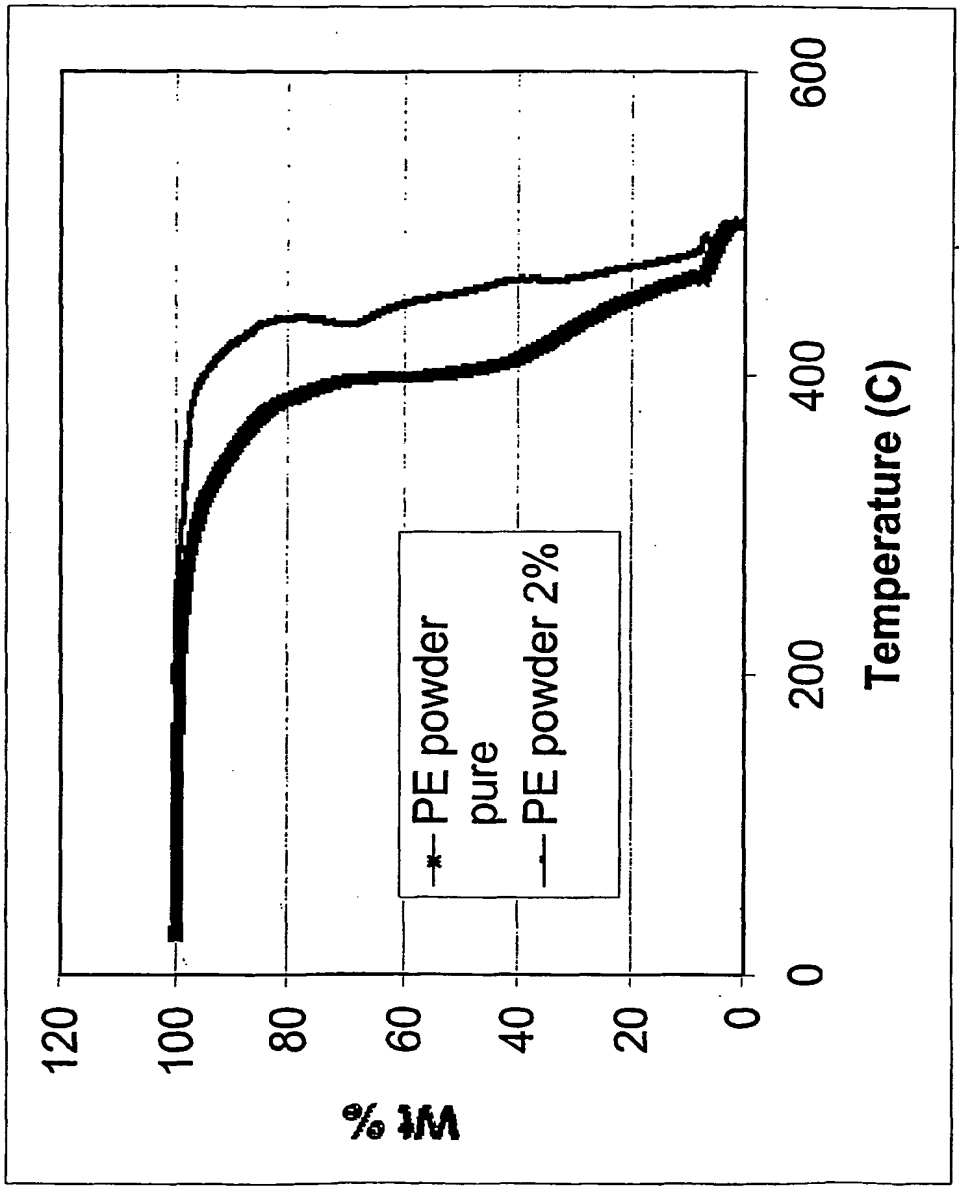

Figure 11 Thermal stability of PE and PE with 2 wt.% HiPco SWNTs. Note that the degradation temperature is 100 C higher for the SWNT filled polymer.

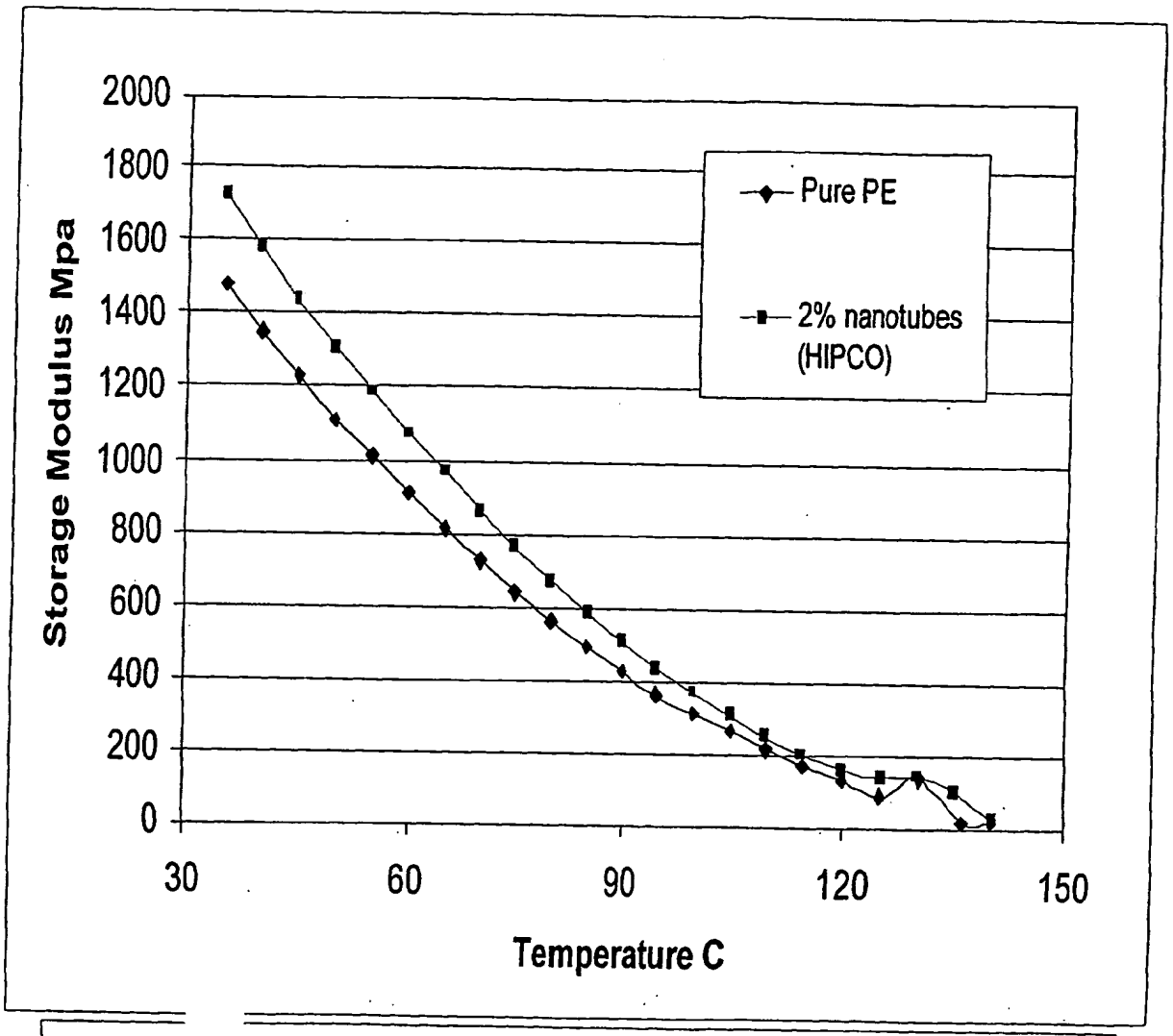

Figure Storage modulus vs. temperature. For PE with and without SWNTs

12

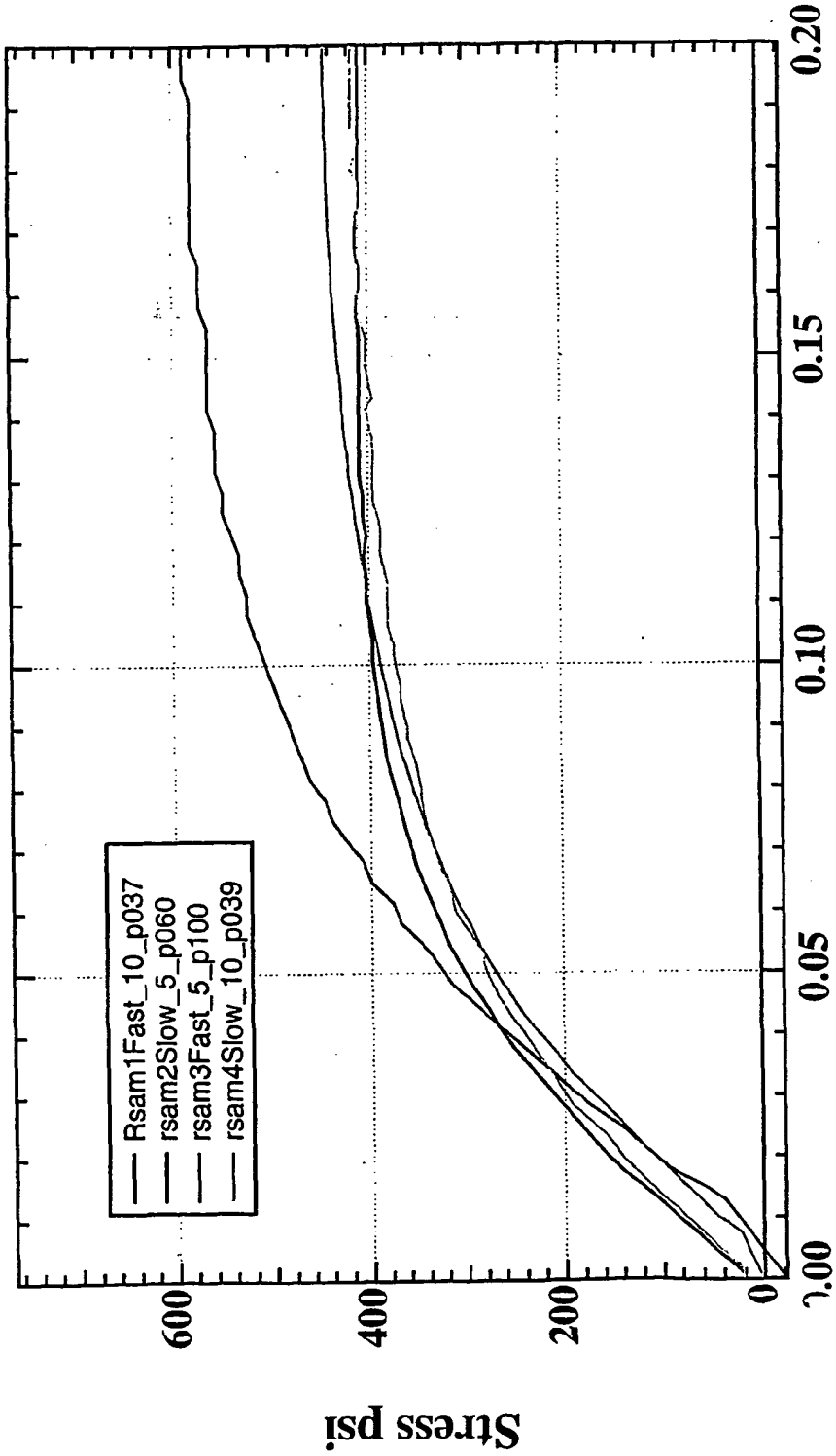

Figure The strength of various fibers when processed at different extruder and take up speeds. Note that high extruder speed coupled to high take up speed leads to stronger fibers.

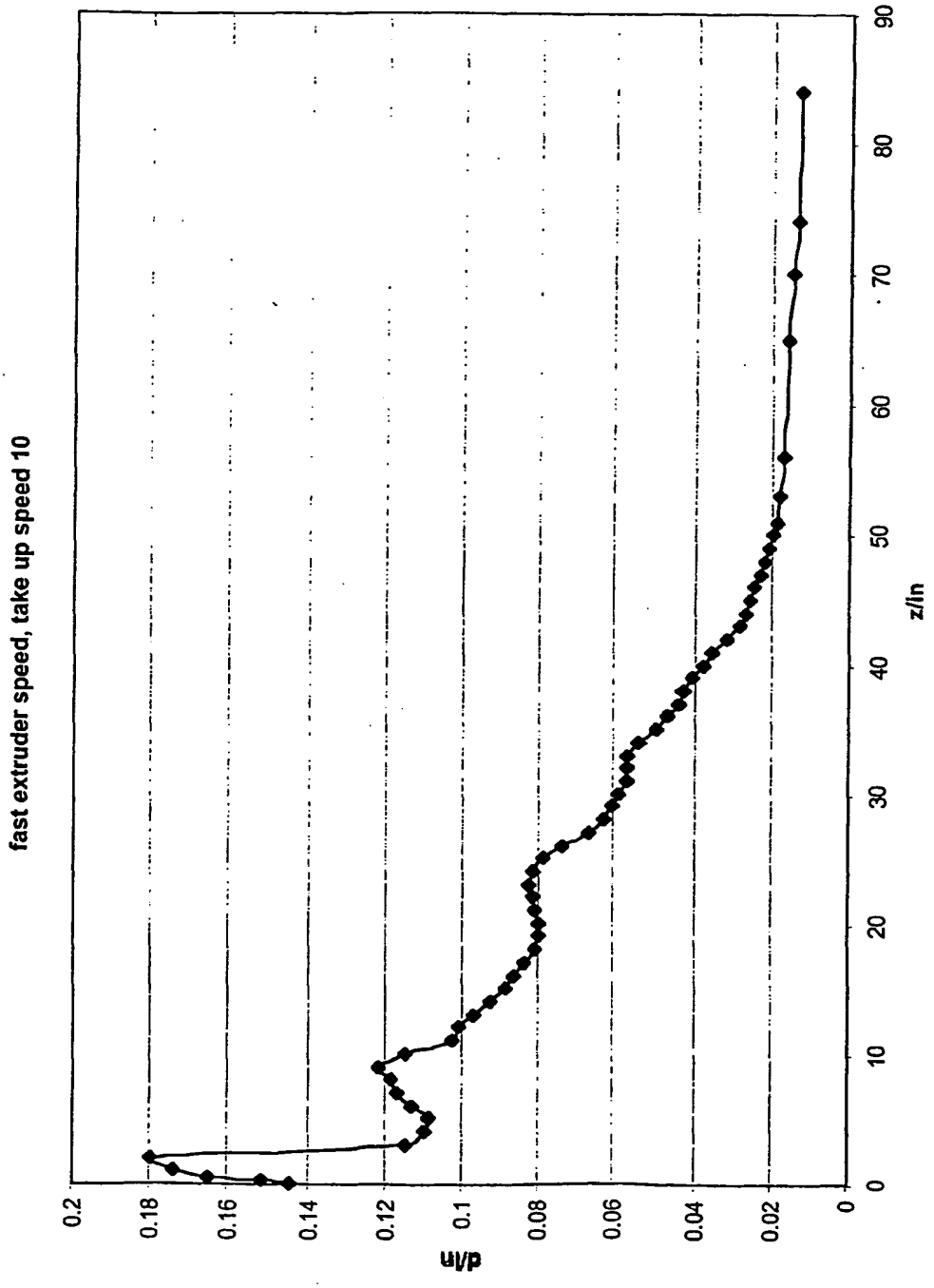

Figure 15 Plot indicating the change in diameter of a fiber system when processed at high extruder speeds and subsequent high take up speeds. Small diameter fibers are sought since defects in these systems tend to be minimized.

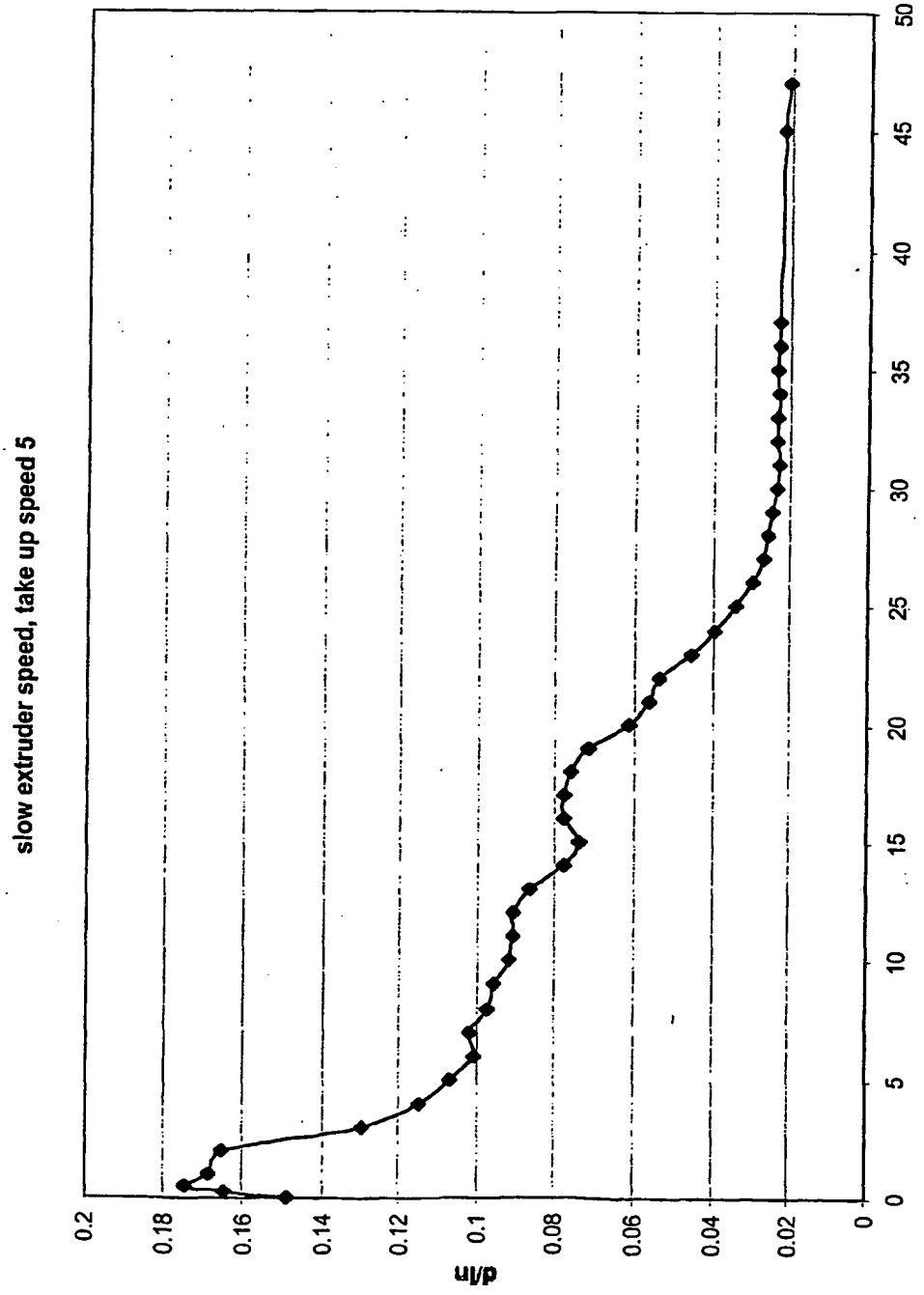

Figure 'lot indicating the change in diameter of a fiber system when processed at slow extruder speeds ana subsequent slow take up speeds. Larger diameter fibers result. This demonstrates that a range of fiber sizes can be processed according to customer needs.

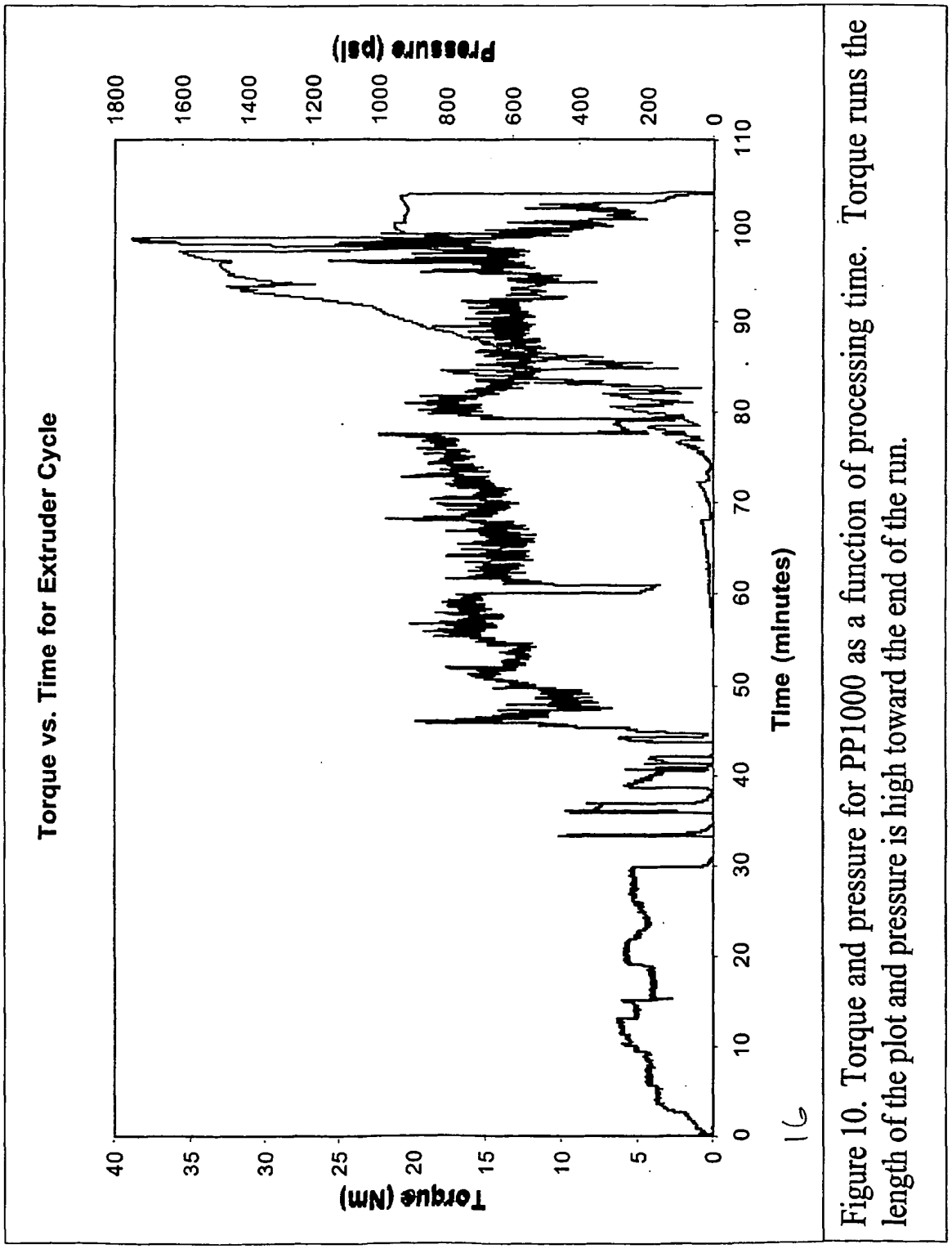

Figure 10. Torque and pressure for PP1000 as a function of processing time. Torque runs the length of the plot and pressure is high toward the end of the run.

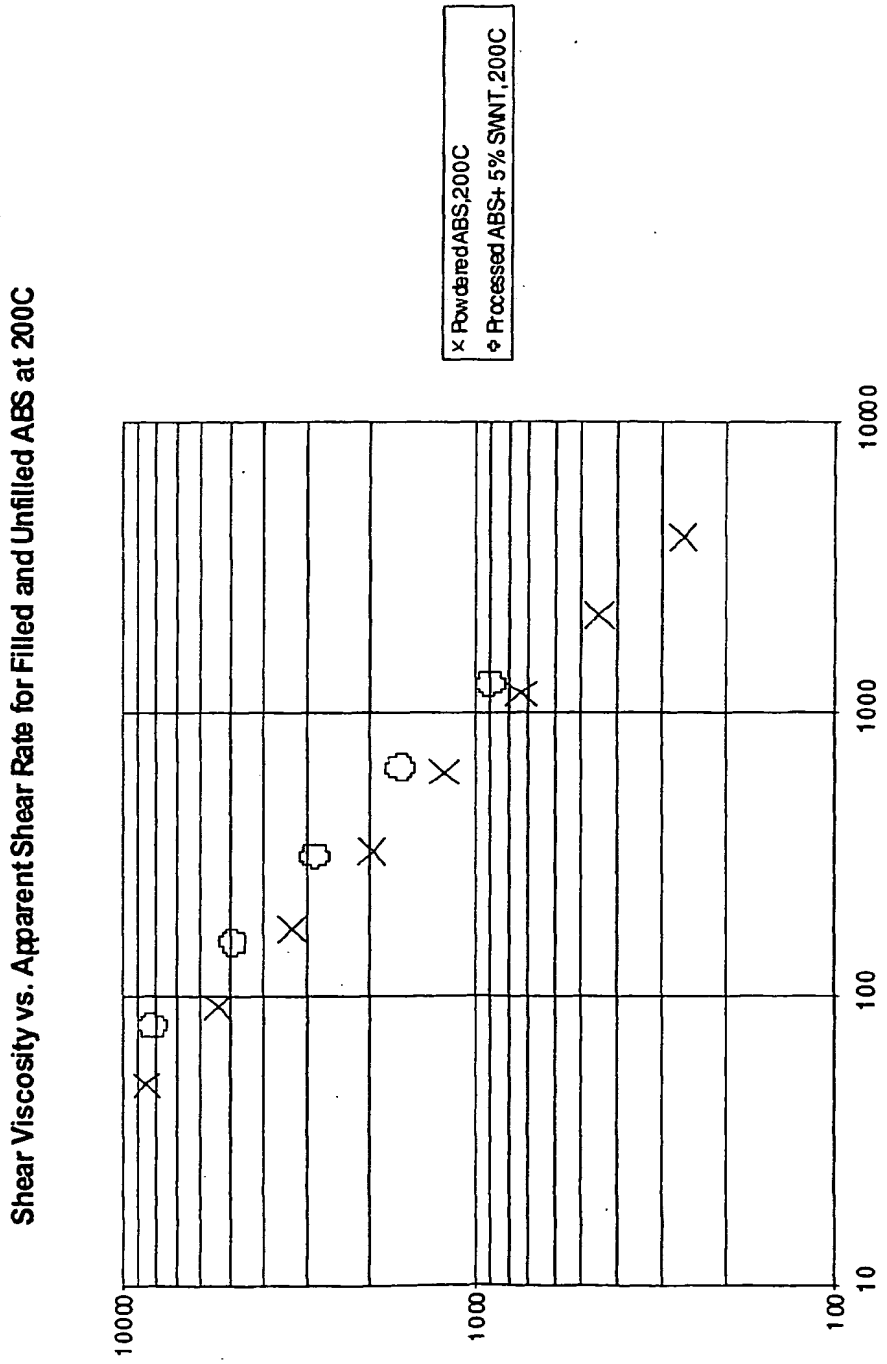

17

Figure Rheological data for melt spinning of ABS. This data helped establish our starting parameters for processing PP and PE with SWNTs.

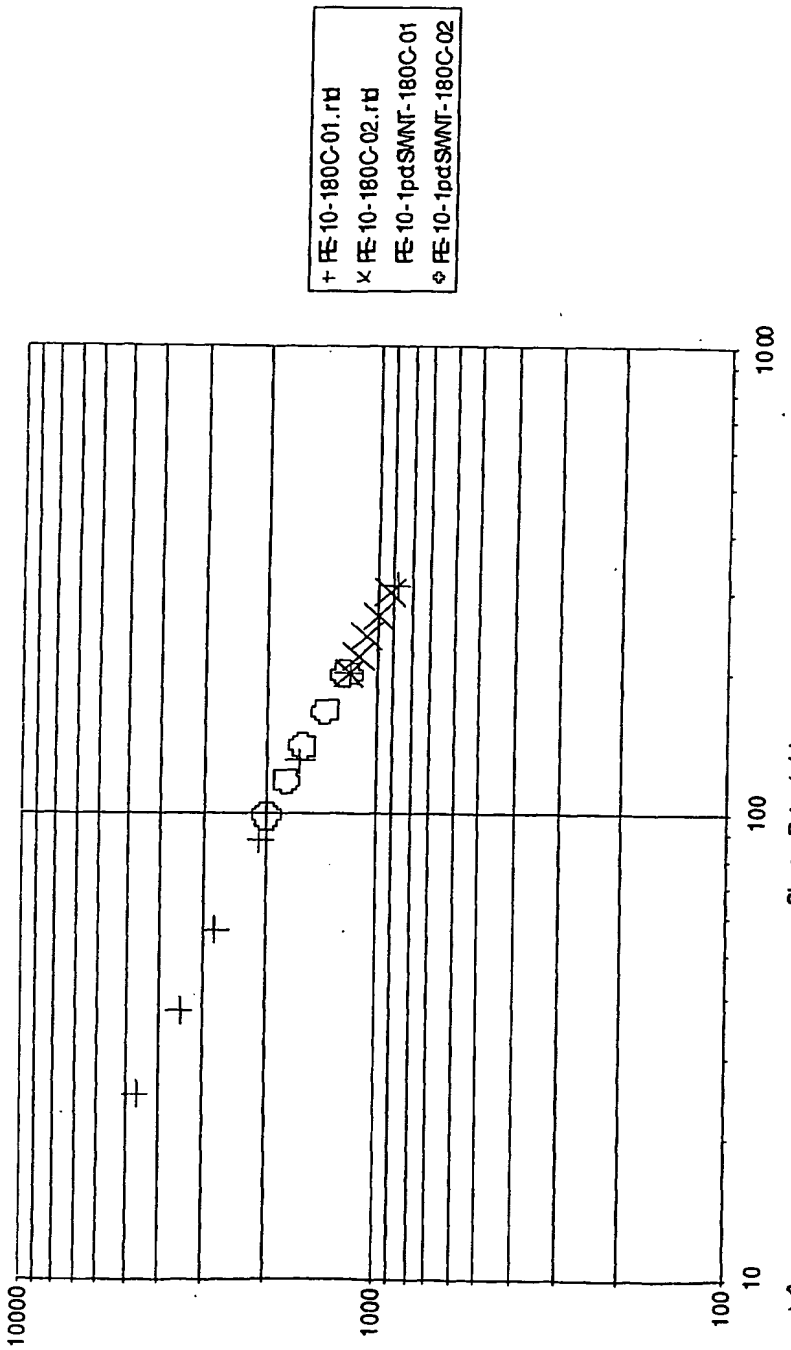

Figure Rheology of PE10 showing the reduced viscosity with increasing shear rate. Note that additions of SWNTs do not increase viscosity at these shear rates.

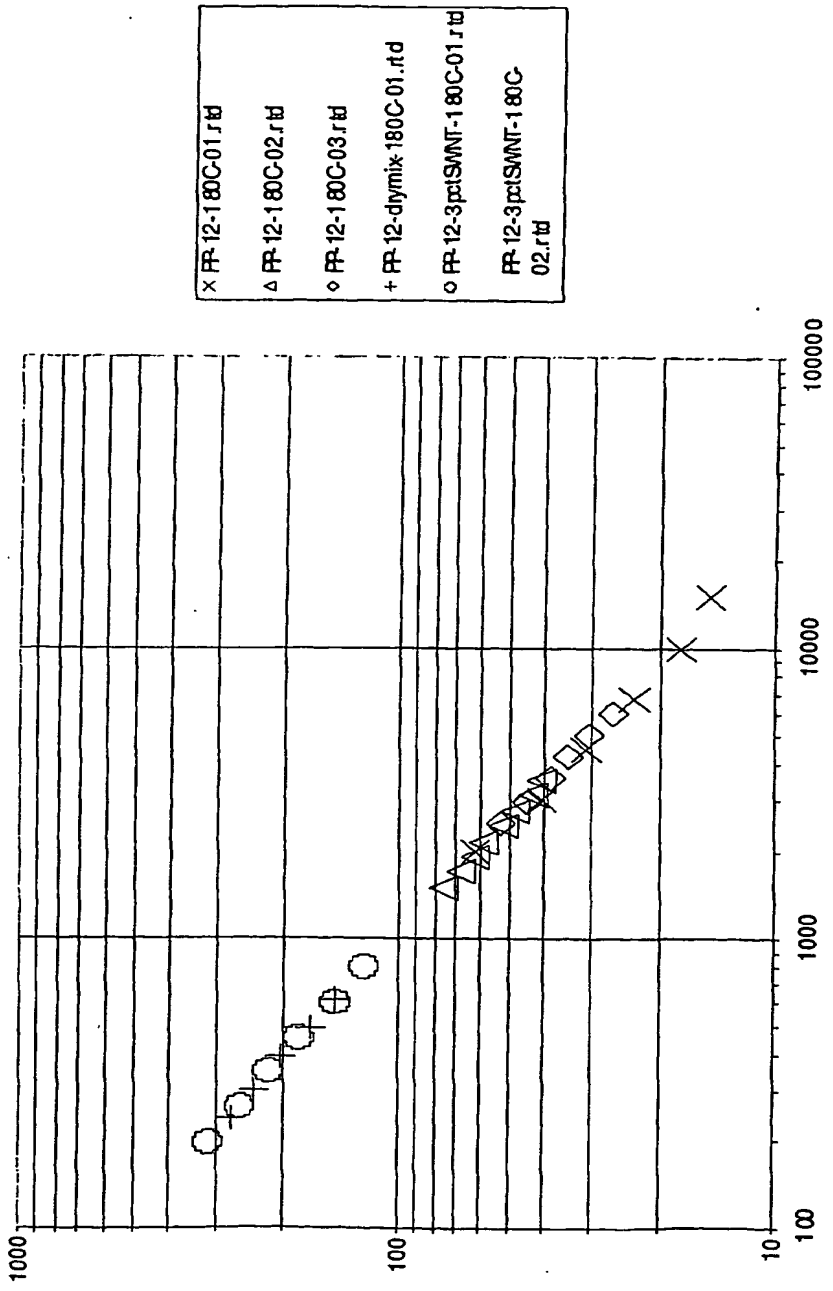

Figure Rheology for PP12 for melt spinning conditions. Note that again the viscosity decreases with increasing shear rate.

20

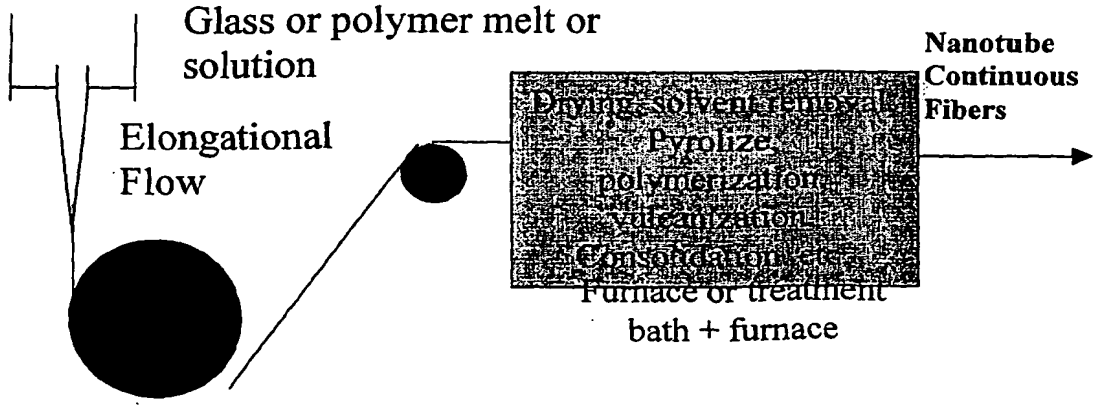
Glass or polymer melt or solution
Elongational Flow
Drying, solvent removal
Pyrolize
polymerization
volatilization
Consolidation
Furnace or treatment bath + furnace
Nanotube Continuous Fibers

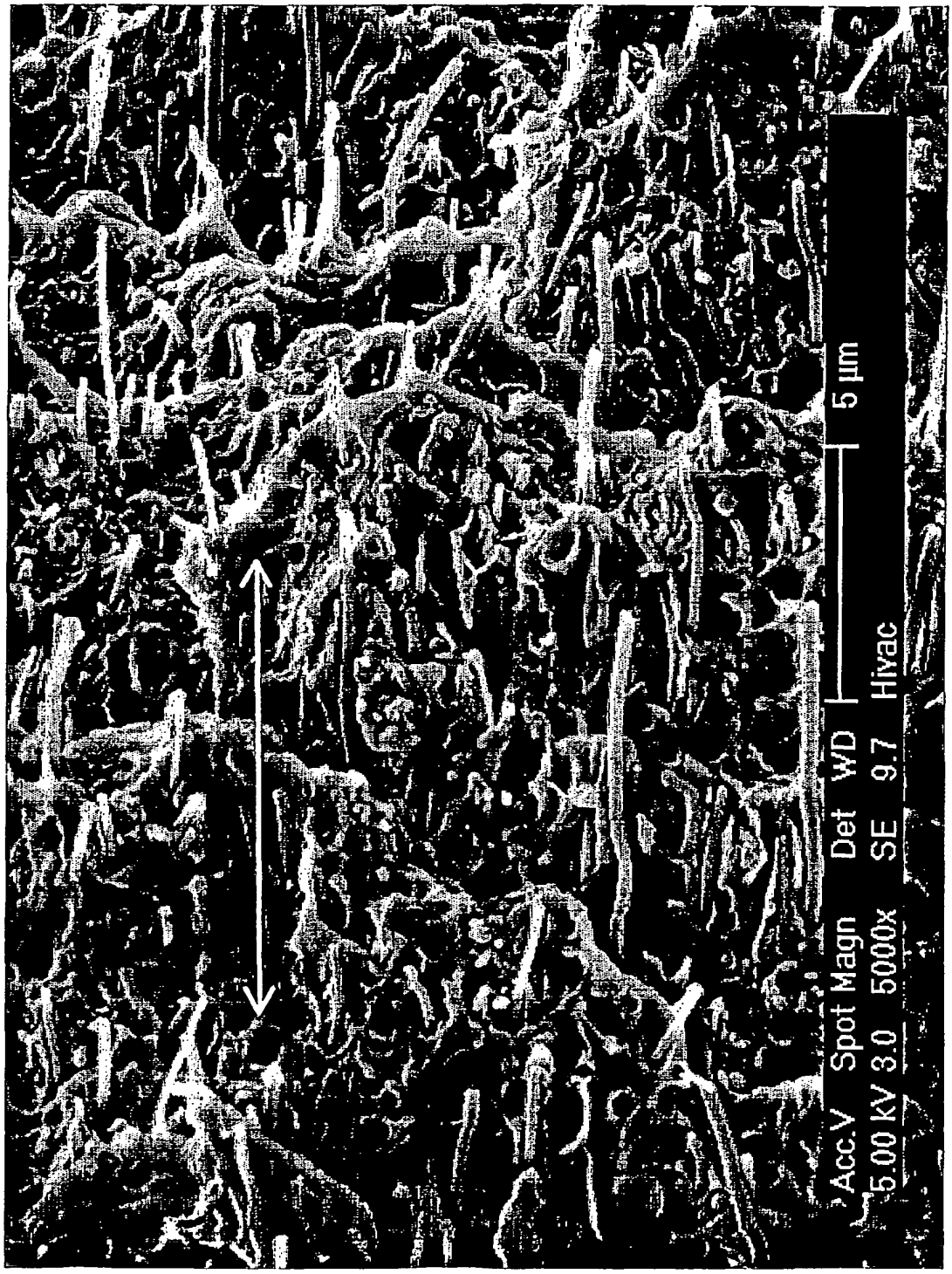

Figure 21. The surface of wire feedstock in the longitudinal direction showing a high degree of VGCF alignment with aspects depicting poor wetting conditions.

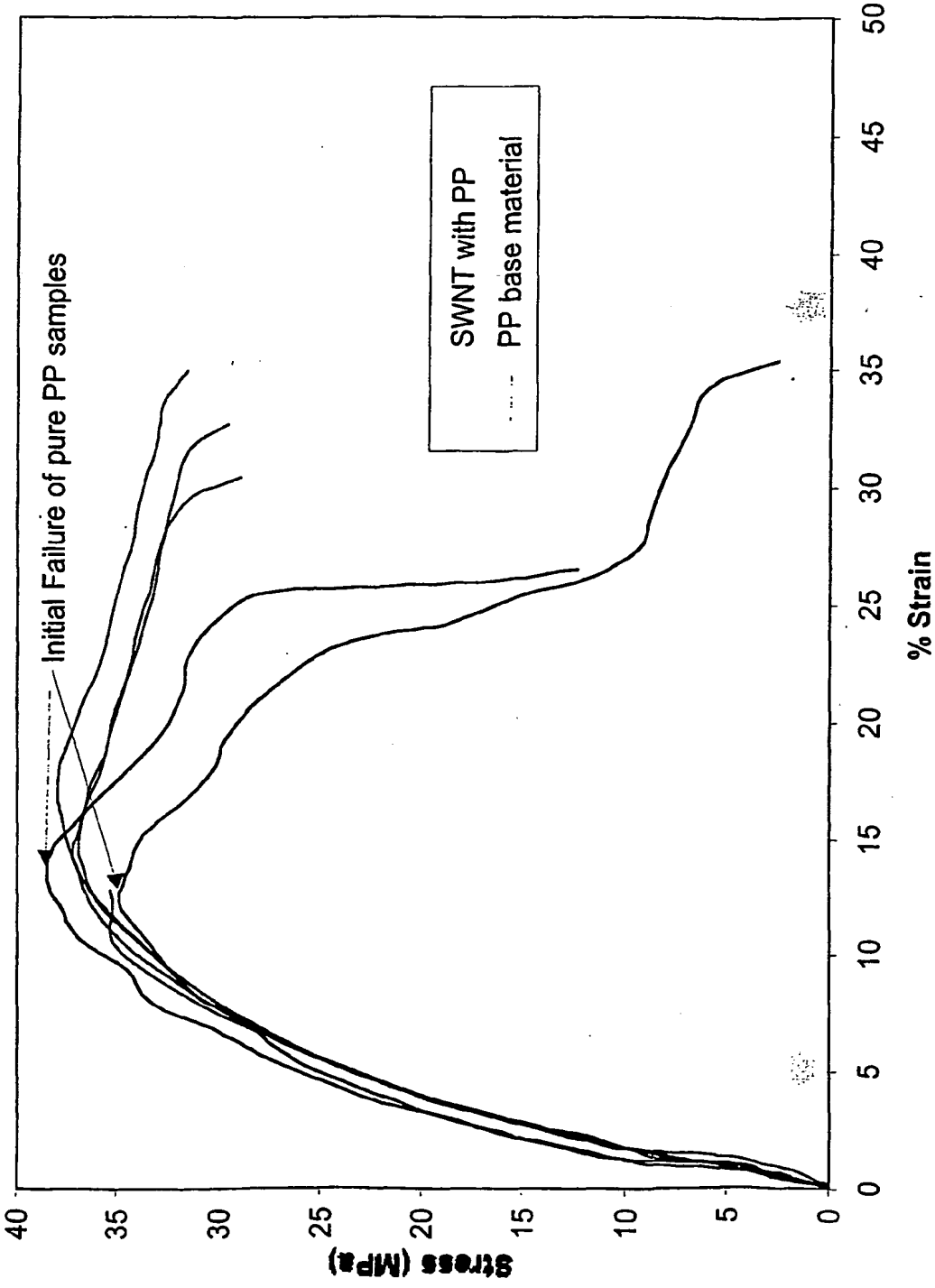

22

Figure Stress-strain curves for PP indicating 115% increase in elongation.

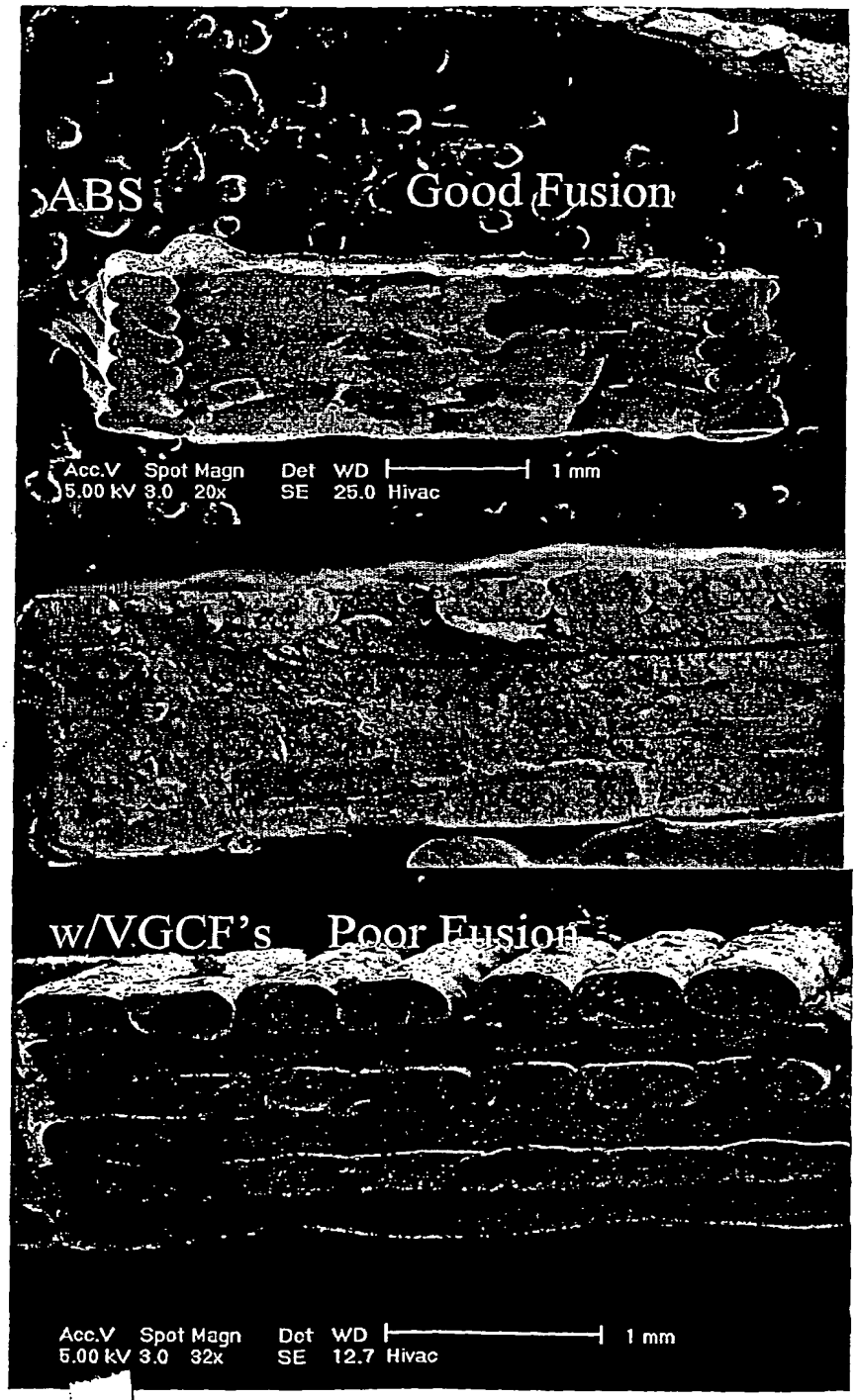

Figure 24 Fracture surfaces of tensile test samples showing incomplete and more complete fusion of the layers and individual FDM traces. Lower shrinkage of the composite material leads to inconsistent fusion of the layers.

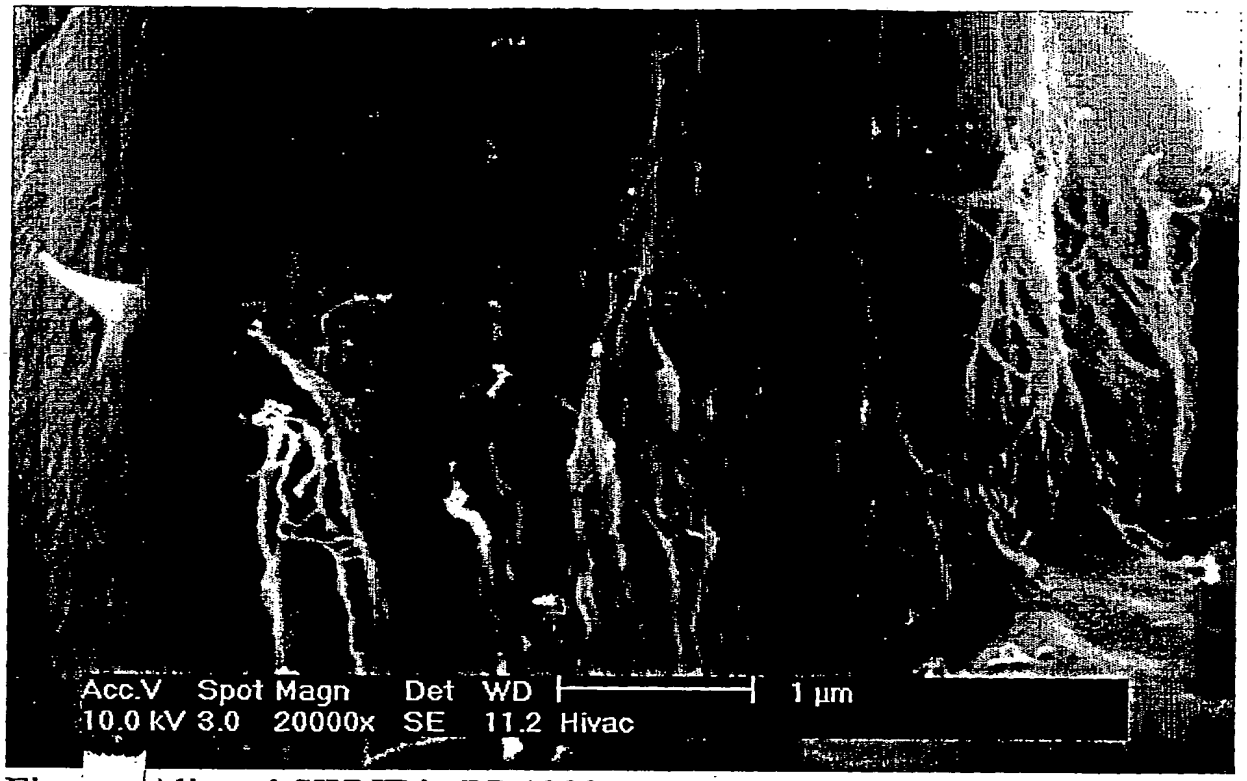

Fig. Aligned SWNT in PP 1200

25

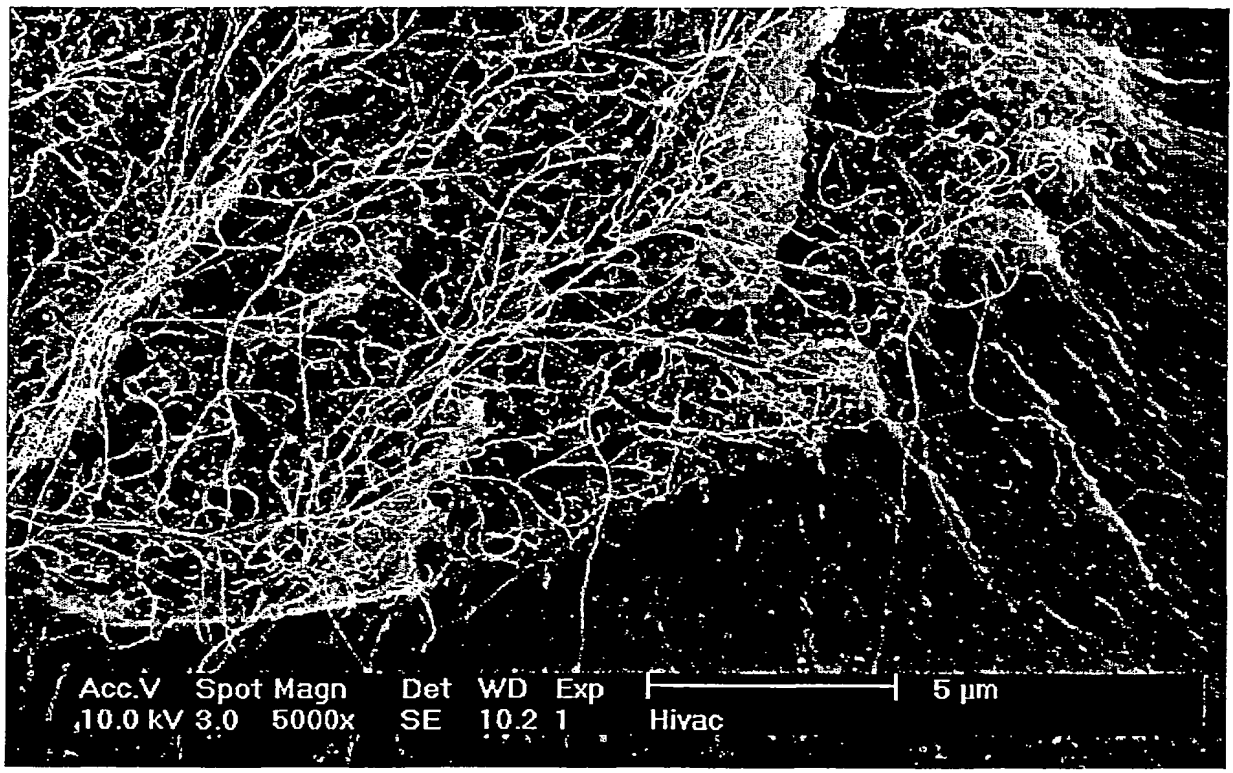

Fig 3a As-Received SWNT do not disperse well

Fig 3a, 3aa

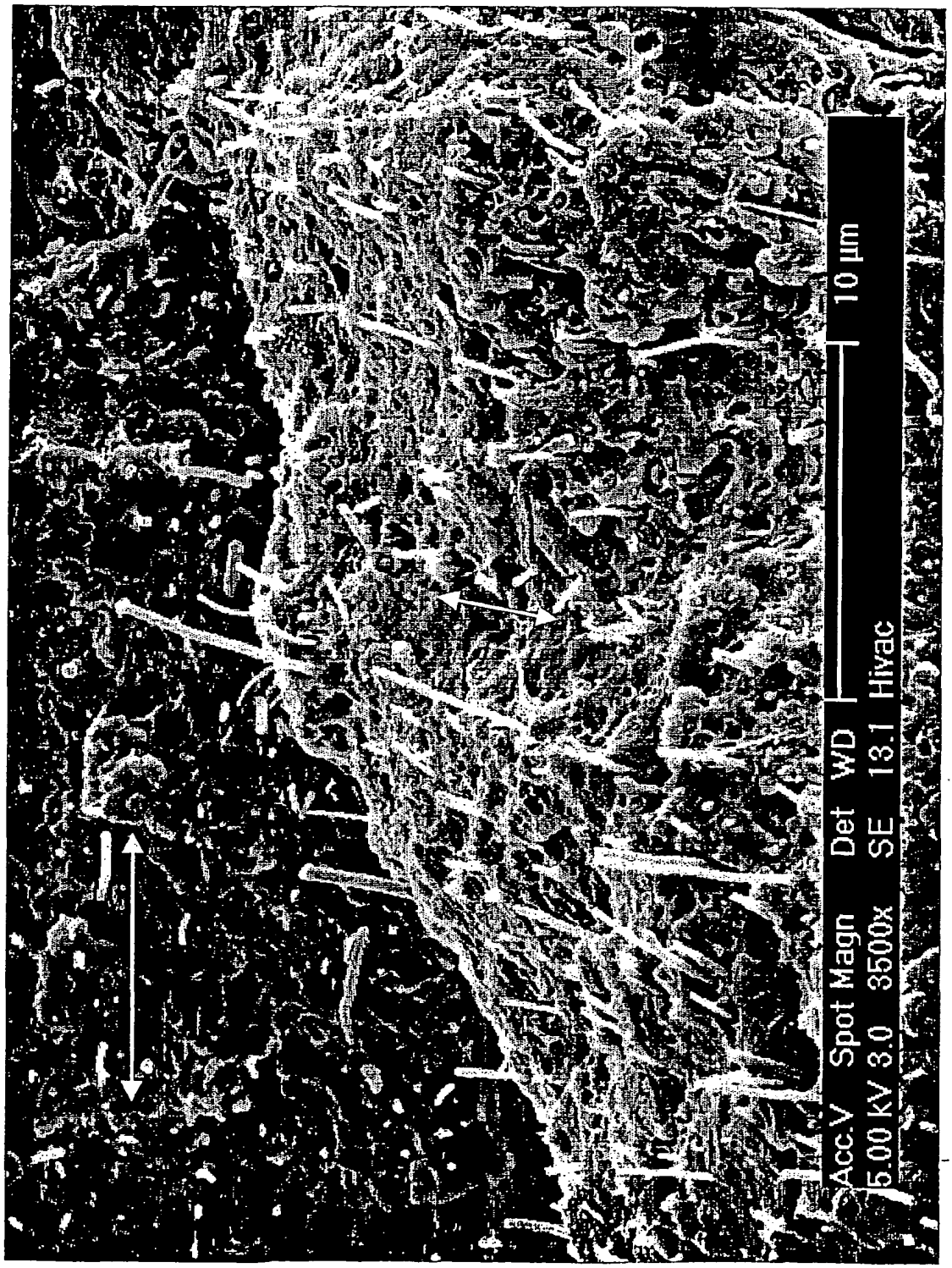

Fig. 33 Intertrace Fusion in cross-ply FDM sample with VGCF oriented in the direction of the wire

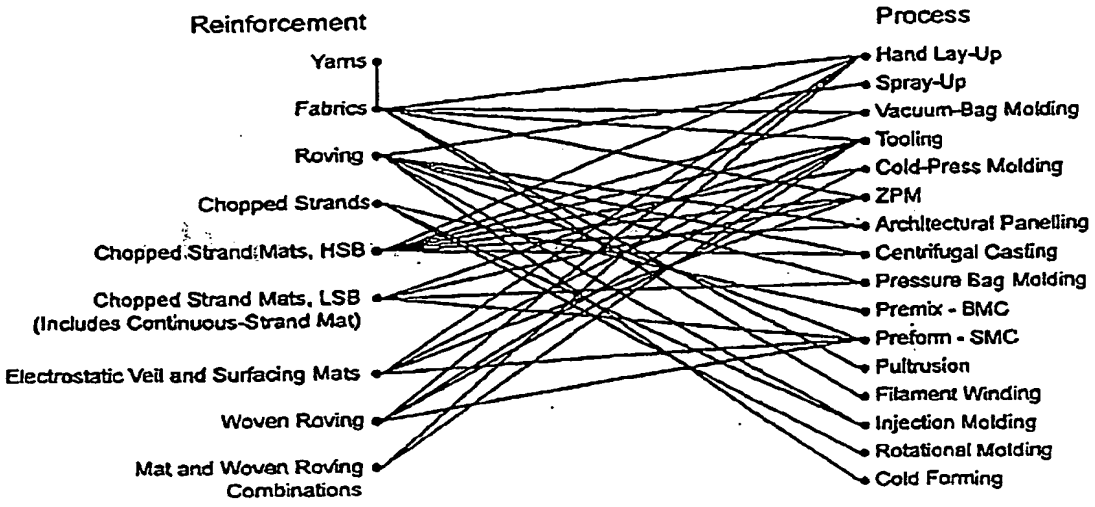

Figure 24 ommercial avenues for nanofiber continuous fibers.

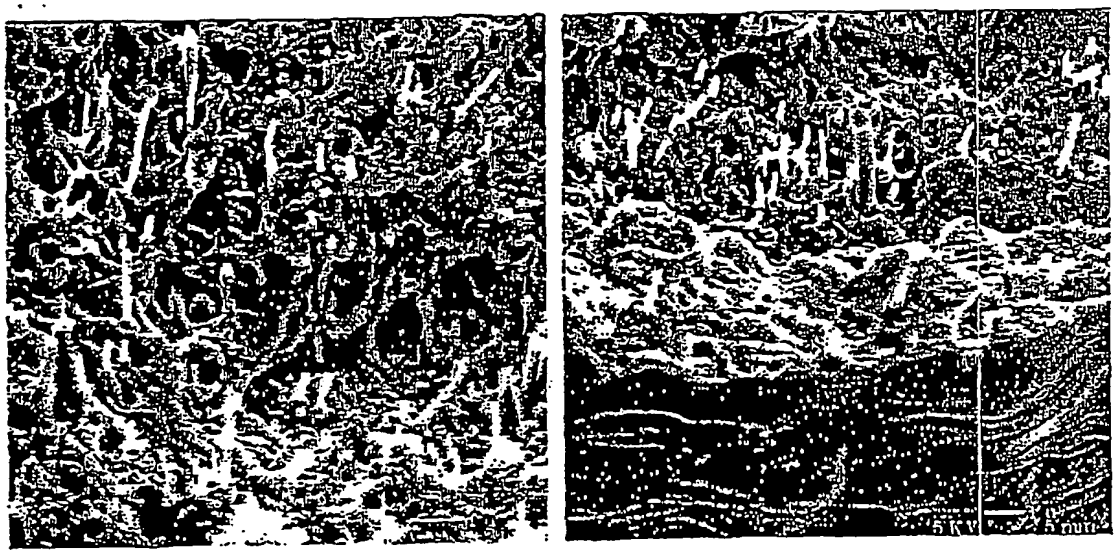

Figure 25. ABS SEM micrographs with dispersed and aligned VGCF (10 wt.%)

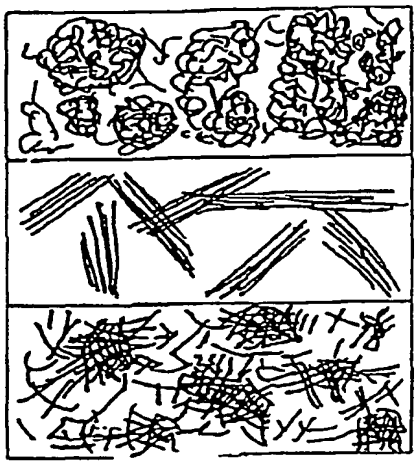

Balling
caused by fiber length too long or fiber mod too low, allowing fibers to ball up in non-interconnecting groups of reinforcements.

Paralleling
caused by poor processing technique or raw material forms such as chopped fiber glass.

Grouping
caused by inefficient mixing, settling out in liquid matrix.

Figure 14. Nanofiber dispersion issues where the initial preparation of the nanofibers may influence the degree of alignment and dispersion obtained.

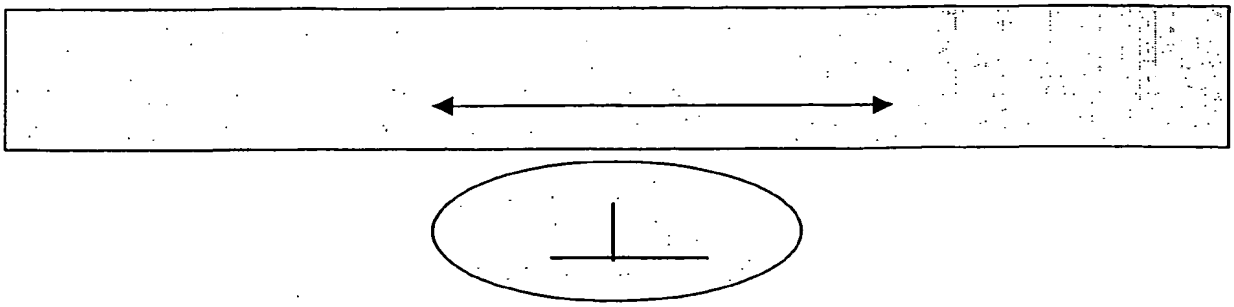

Figure 34 Schematic showing a 90°/180° orientation of FDM traces in a tensile sample. The + indicates the trace is in the direction of the tensile axis and the arrows indicate the trace is aligned perpendicular to the applied load.

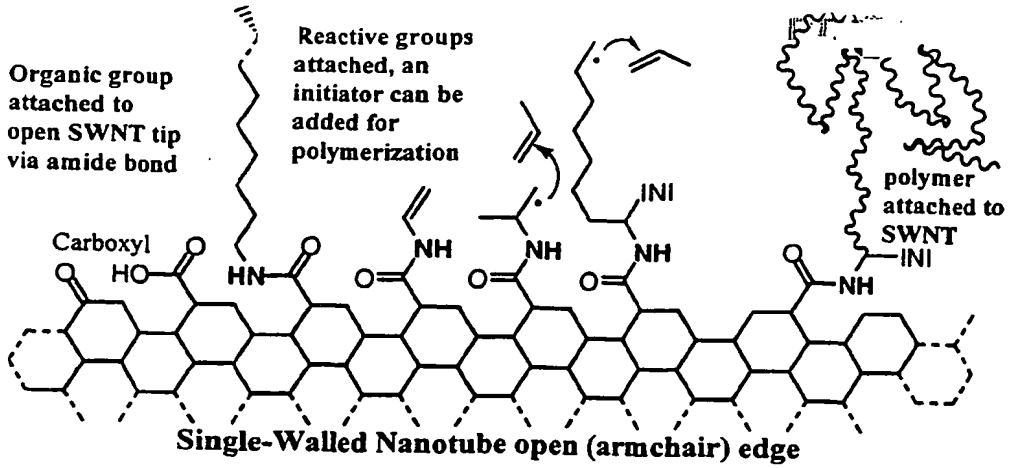

Fig 35

as exemplified in Figure 2.

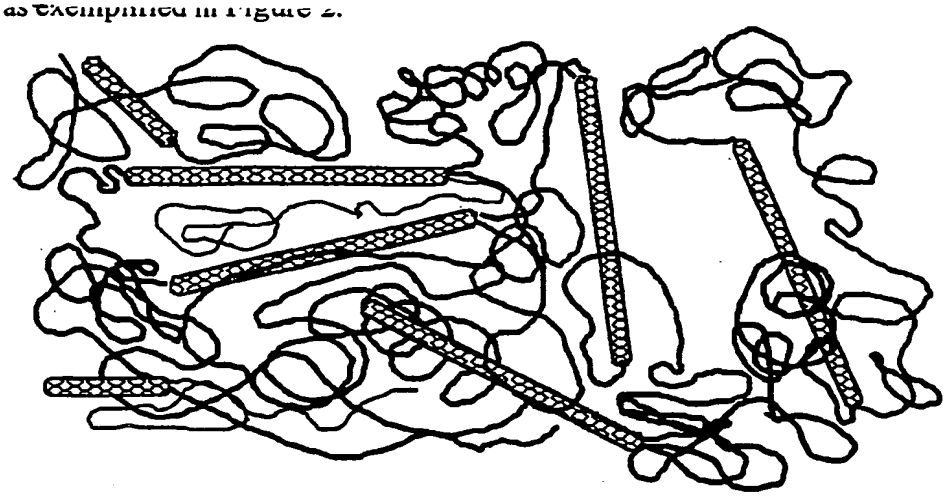

Fig 36

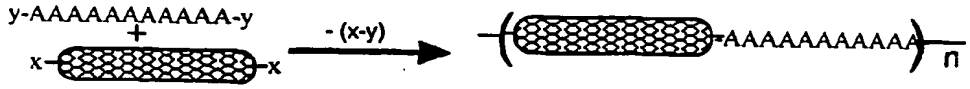

Fig 37

Figure 3: Representation of nanotube block co-polymers.

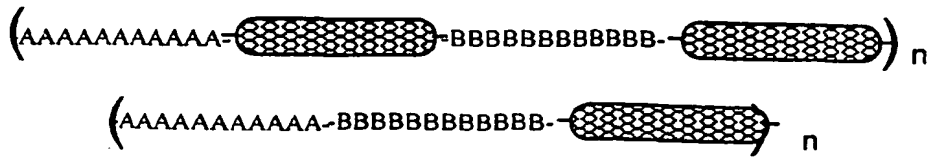

Fig 38

Figure 4. Nanotube block co-polymers, with two different configurations possible for alternating polymer blocks.

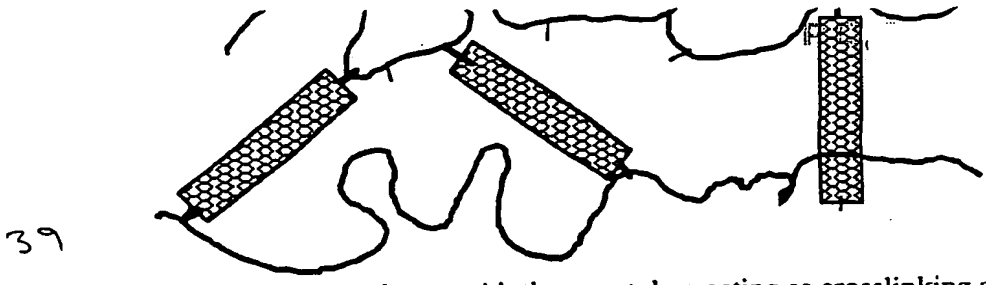

Figure 5: Nanotube graft copolymer with the nanotubes acting as crosslinking agents.

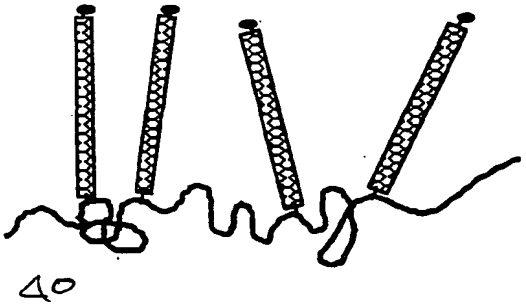

Figure 6: Nanotube graft copolymer where only one side of the nanotube can attach to the polymer chain.

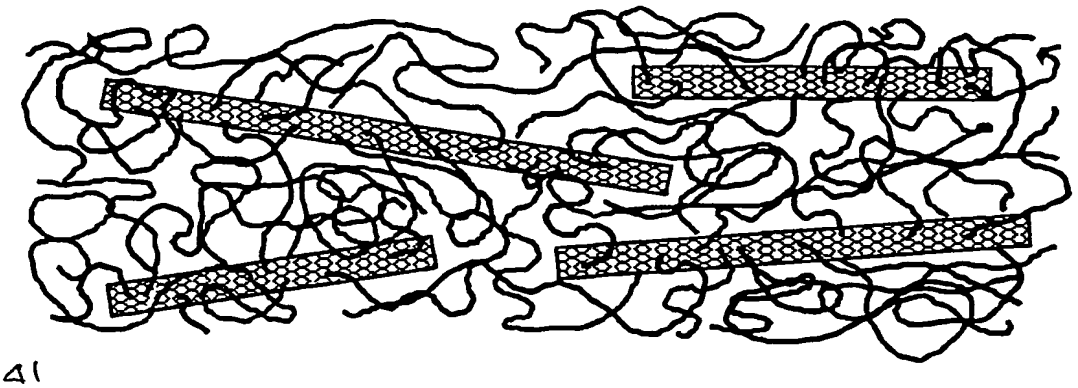

41

Figure 9. Side-wall attached polymer-nanotube composite, with random polymerization creating crosslinking.

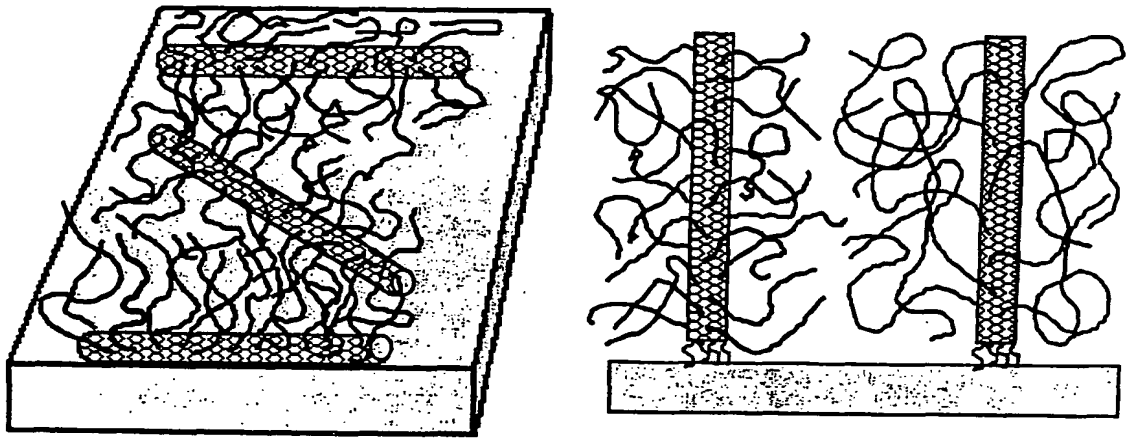

42

Figure 10. "Hairy-tube composites". Left side: SWNTs over a substrate, only the exposed surface is covered with polymer. Right side: Tips of SWNTs attached to a solid support, with the possibility of controlling the length and crosslinking of the polymer chains.

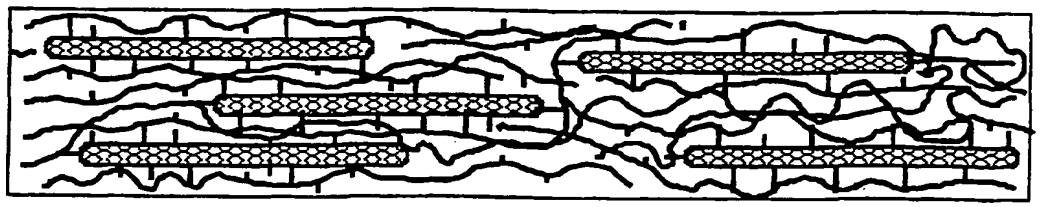

43

Figure 11: Nanotubes shear oriented and then chemically bonded to the polymer matrix.

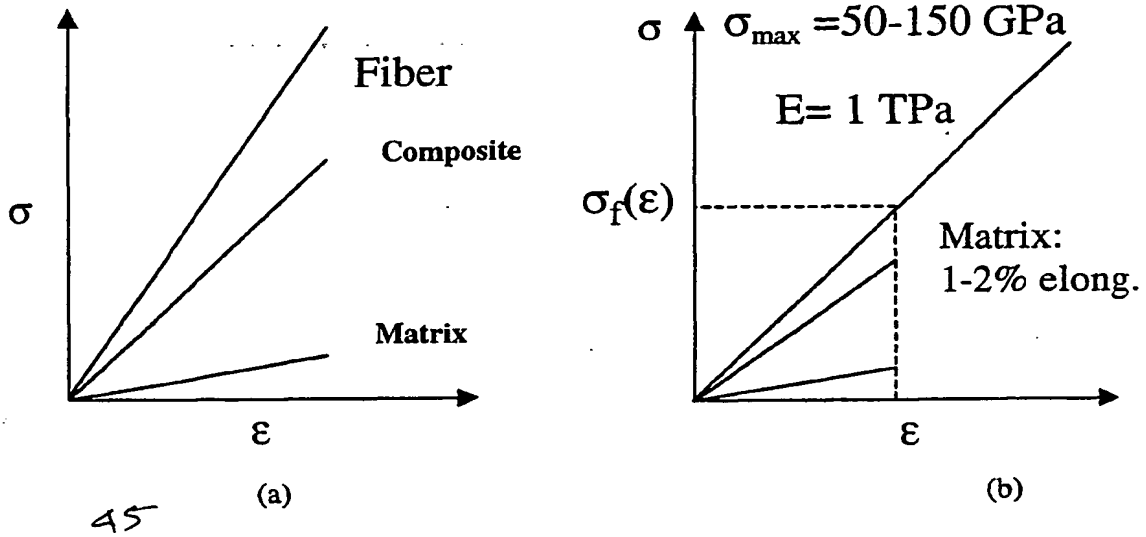

45

Figure 19. Comparison of a stress-strain curve for (a) a typical epoxy composite compared to that for (b) a nanotube composite where significant strength of the nanotube is discarded. SWNTs are expected to have a high degree of elongation to failure.

Fig 46

Table 4: Parameters used to calculate the properties of SWNT composites by Rule of Mixture Calculations based on an ABS polymer as the mnatrix.

Parameters	Value	Source
SWNT Diameter	1.4 nm	A. G. Rinzler, J. Liu, H. Dai, P. Nikolaev, C. B. Huffman, F. J. Rodriguez-Macias, P. J. Boul, A. H. Lu, D. Heymann, D. T. Colbert, R. S. Lee, J. E. Fischer, A. M. Rao, P. C. Ecklund, and R. E. Smalley, Appl. Phys. A **67**, 29 (1998).
SWNT Length	300 nm	Per Barrera/Smalley Conversation
SWNT Rope Diameter	10 nm	J. P. Salvetat, G. A. D. Briggs, J. M. Bonard, R. R. Basca, A. J. Kulik, T. Stockli, N. A. Burnham, and L. Forro, Phys. Rev. Lett. **82**, 944 (1999).
SWNT Rope Length	6μm	J. P. Salvetat, G. A. D. Briggs, J. M. Bonard, R. R. Basca, A. J. Kulik, T. Stockli, N. A. Burnham, and L. Forro, Phys. Rev. Lett. **82**, 944 (1999).
SWNT Tensile Strength	50 GPa	H. D. Wagner, O. Lourie, Y. Feldman, and R. Tenne, Appl. Phys. Lett. **72**, 188 (1998).
SWNT Rope Tensile Strength	13 GPa	M. F. Yu, B. S. Files, S. Arepalli, and R. S. Ruoff, Phys. Rev. Lett. **84**, 5552 (2000).
SWNT/ABS Interfacial Strength	500 MPa	H. D. Wagner, O. Lourie, Y. Feldman, and R. Tenne, Appl. Phys. Lett. **72**, 188 (1998).
SWNT Rope Shear Strength	6 MPa	P. M. Ajayan, L. S. Schadler, C. Giannaris, and A. Rubio, Adv. Mat. **12**, 750 (2000).
SWNT Density	1.39 g/cm^3	Calculated
ABS Density	1.04 g/cm^3	Sigma-Aldrich Chemical Company
ABS Tensile Strength	22.8 MPa	Experimentally measured

64

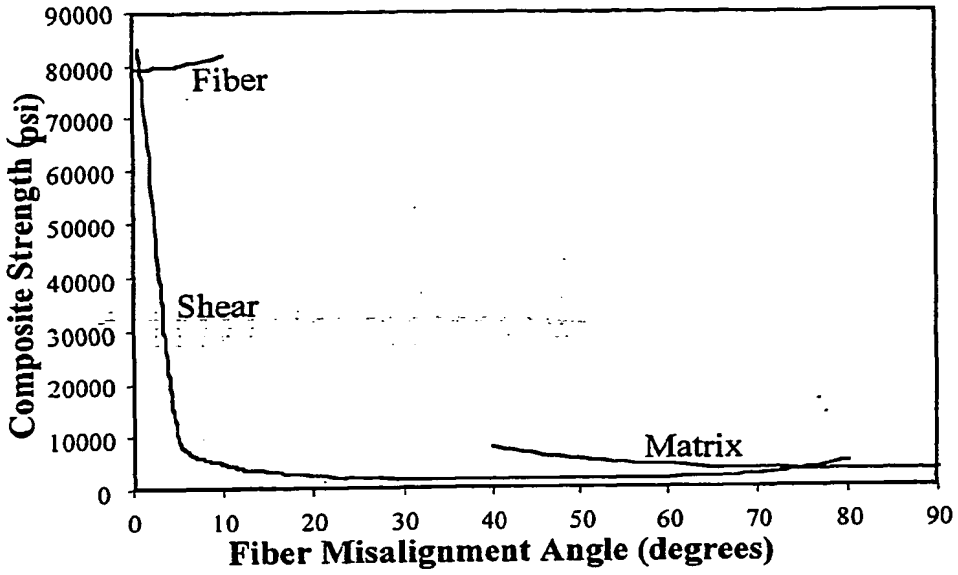

Figure 11. Composite strength vs. the orientation of the SWNTs when considered to be fully aligned. Note that initially when all fibers are aligned with the applied load the strength of the composite is rather high. As the fibers become misoriented with the load (as in the case of an isotropic composite where SWNTs are randomly dispersed), the composite strength goes way down due to low shear and normal strength contributions. On one hand you might use convential processing to improve the shear and normal stresses where as we take the approach to fully integrate and therefore remove defects that might also result in the matrix.

Table 1. Properties of VGCFs and ABS

VGCF Properties	**Polygraph III**
Magnum ABS	**GMID #31875**
Tensile strength (psi): 5,000	Elongation (%): 50
Flexural strength (psi): 9,500	Hardness (Shore D): R105
Tensile modulus (psi): 360,000	Softening point (R&B)(F): 220
Flexural modulus (psi): 380,000	Specific gravity (GMS/cm^3): 1.05
Notched impact (ft ib/in): 2.00	

Table 2. Tensile Data for SWNT/ABS FDM Composites.

Sample No.	Peak Load (lb)	Cross sectional area (in^2)		*Stress (psi)	Strain to break (%)	Modulus (kpsi)
1	40.2	0.0178	2260	1.7	118	
2	49.2	0.0171	2876	1.7	179	
3	45	0.0178	2540	1.7	160	
4	57.2	0.0192	2978	1.7	204	
5	50	0.0187	2719	1.7	136	

*Stress values are based on measured starting areas and not on actual tests areas due to incomplete fusion.

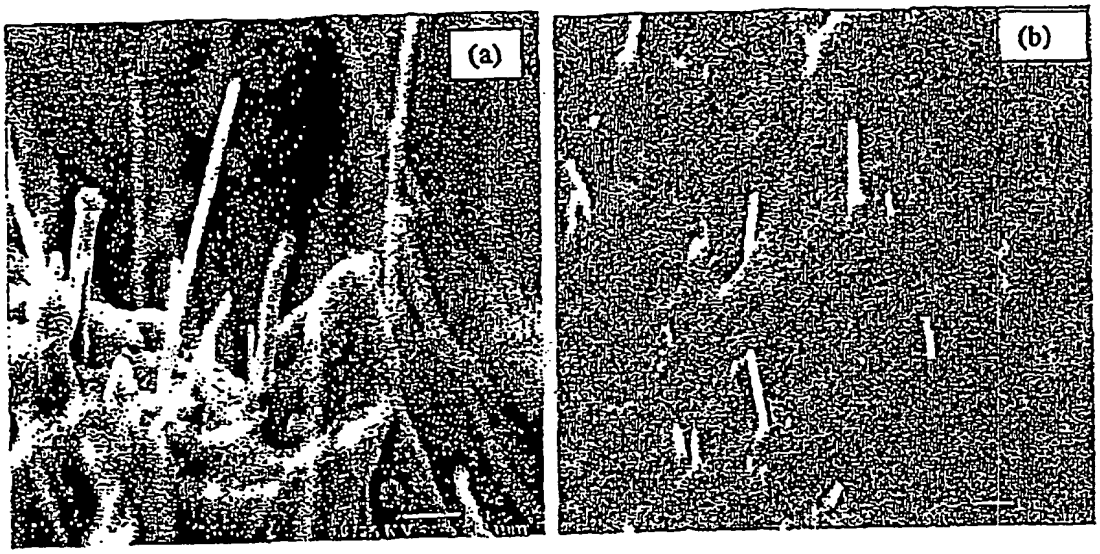

Figure 9. PE with dispersed and aligned VGCF (a) 5wt.% and (b) 2wt.%.

26

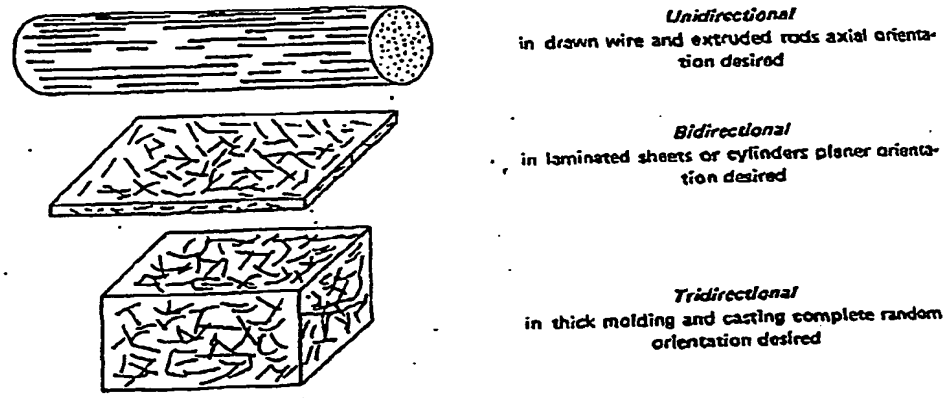

Figure 10. Desired nanofiber alignment by inducing directionality by shearing into forces

27

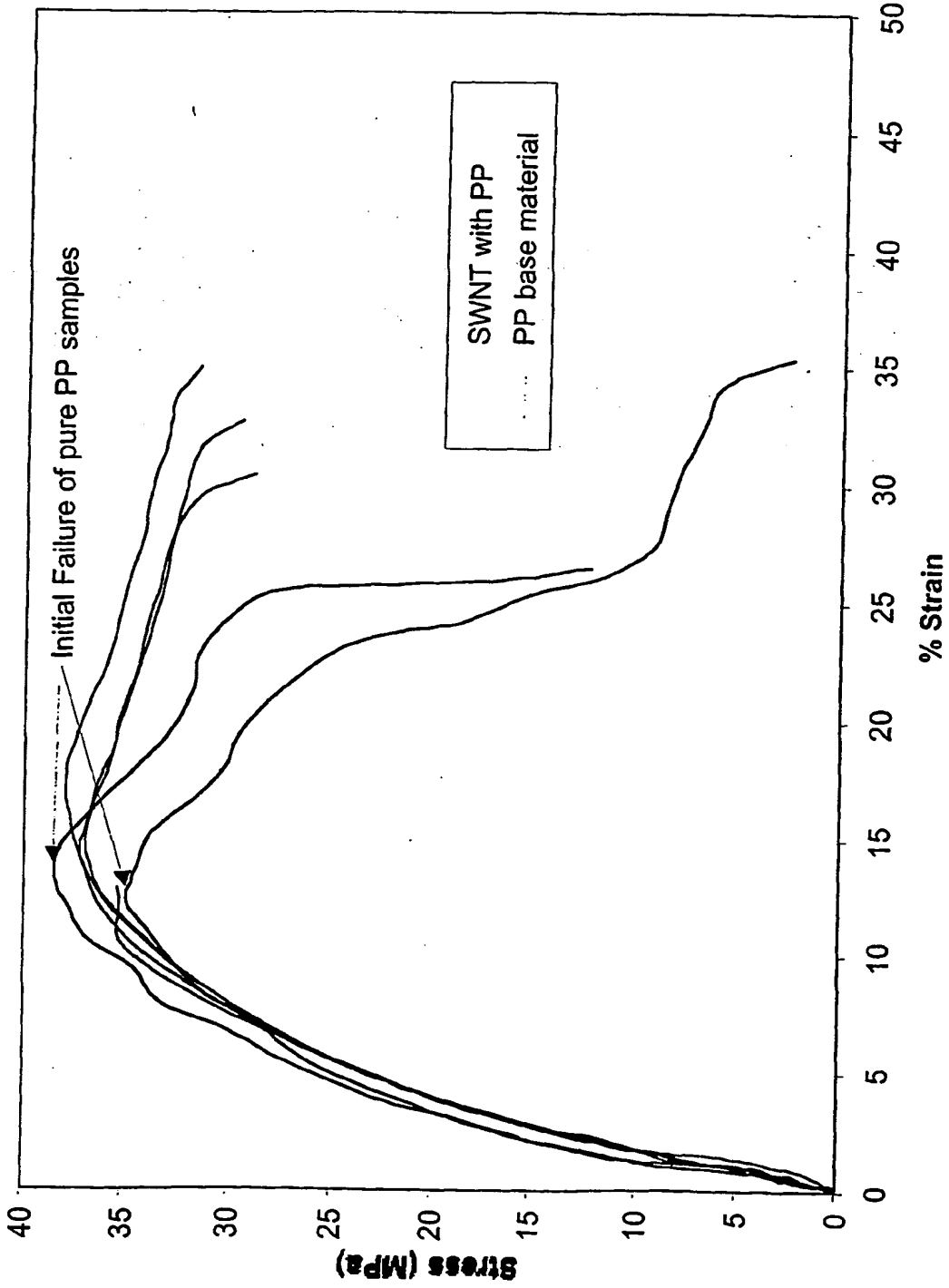

Figure Stress-strain curves for PP indicating 115% increase in elongation.

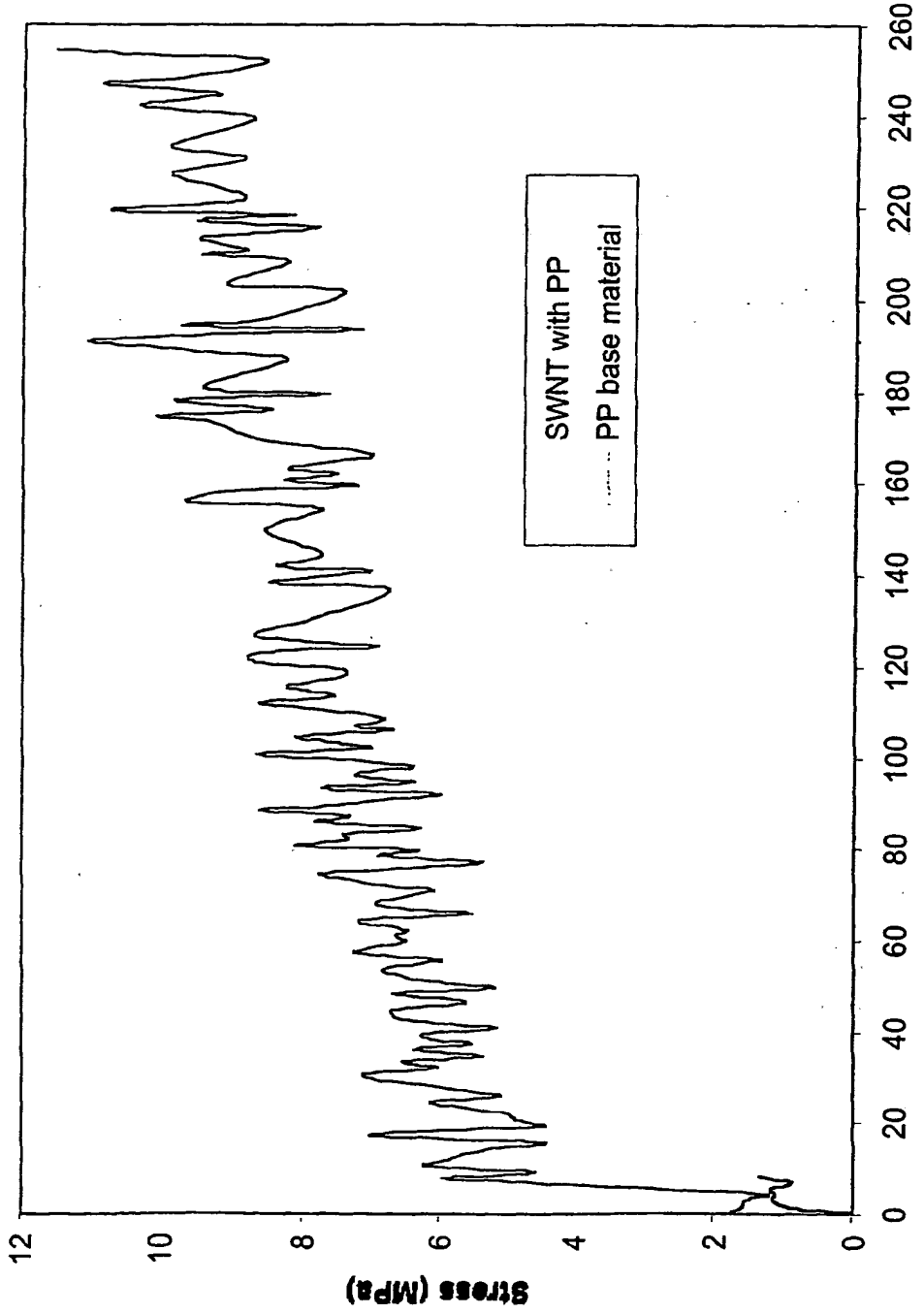

Figure Stress-strain curves for PP fibers showing increases in tensile strength by 743% and elongation to failure by 2964%. Recently an investigator at Georgia tech was extremely excited by the potential of achieving such improvements in fiber conditions.